Ship collision analyses based on finite element and super-element methods

Auteur : Moran Arellano, Jonathan Alexander
Promoteur(s) : 14958
Faculté : Faculté des Sciences appliquées
Diplôme : Master : ingénieur civil mécanicien, à finalité spécialisée en "Advanced Ship Design"
Année académique : 2020-2021
URI/URL : http://hdl.handle.net/2268.2/13304

Ship collision analyses based on finite element and super element methods

submitted on 23 August 2021

by

MORÁN ARELLANO Jonathan Alexander

37 rue du Champ de Manoeuvres

44470 Carquefou

jonalex_ec@hotmail.com

Student ID No.: s193103

Supervisor:

Professor LE SOURNE Hervé

ICAM site de Nantes

35 avenue du champ de manoeuvre

44470 Carquefou

France

Reviewer:

Professor RIGO Philippe

University of Liège, ANAST

Allée de la Découverte 9

4000 Liège

Belgium

CONTENT

Declaration of Authorship

I declare that this thesis and the work presented in it are my own and have been generated by me as the result of my own original research.

Where I have consulted the published work of others, this is always clearly attributed.

Where I have quoted from the work of others, the source is always given. Except for such quotations, this thesis is entirely my own work.

I have acknowledged all main sources of help.

Where the thesis is based on work done by myself jointly with others, I have made clear exactly what was done by others and what I have contributed myself.

This thesis contains no material that has been submitted previously, in whole or in part, for the award of any other academic degree or diploma.

I cede copyright of the thesis in favour to Universidad Politécnica de Madrid

Date: Signature

This page was intentionally left blank

ABSTRACT

In the current work is presented a comparison of non-right-angle ship-ship collision events generated with numerical simulations based on nonlinear explicit finite element method and super-element method. The purpose is to analyse the limitations of the two approaches when non-perpendicular collisions occur on the side structure of a ship which is not considered at rest. Besides, facing the importance of the inclusion of crashworthiness analysis in ship construction, a first analytical tool for the pre-design stage is proposed in collaboration with the shipyard Chantiers de L'Atlantique in the second part of this document.

Since ship collisions are considered as the most hazardous accidental state, it is first highlighted the attempts of the research marine structure community in the understanding of this event. The literature about numerical analysis of ship collision is reviewed to find the existing procedures to assess the resistance force of structures subjected to impact loads. The relation between the existing methods is presented as well as the current limitations in the field of collision of ship structures. It is found the requirements from the Classification Societies regarding ship collision and grounding are still at a low level of assessment.

A recent benchmark collision study is used for the validation of parametrized collision scenarios made up with LS-Dyna. The setup of the simulation file is described considering the association with the MCOL code to assess the rigid body dynamics of the ships, finding differences due to the rupture criteria assumed. Non-right-angle collisions were generated considering the struck ship has initial velocity and the damage is evaluated with the side penetration and the internal energy dissipated. The same collision scenarios are reproduced with the super-element-based SHARP program and the comparison of results is analysed. It was found how the closed-form expression of the SHARP program limits the deformation energy contribution from other elements that according to LS-Dyna are deforming in the process. The sliding energy was found to be more important in narrow collision angles when both ships have opposite directions.

An analytical tool based on a shared-energy design procedure is also proposed for the pre-design stage of impact loads in the ship construction. The deformation energy obtained by the damaged volume in the crushing process of both deformable ships is expected to be like the initial kinetic energy mainly influenced by the initial velocity of the striking ship. A threshold value for the velocity of the striking ship is estimated from the maximum penetration expected in the struck ship to avoid a large-scale explosion event. Simulations in LS-Dyna are generated to find the influence of the damage due to a high-velocity impact and to the striking ship bow.

RESUMEN

En este trabajo se presenta una comparación de colisiones no perpendiculares de buques utilizando simulaciones numéricas basadas en el método de elementos finitos explícito no lineal y el método de super elementos. El fin es analizar las limitaciones de los dos enfoques en el caso de colisiones no perpendiculares que afectan el costado de un barco en movimiento. Además, contemplando la importancia de evaluar la resistencia a colisiones, en una segunda sección de este documento se busca proponer una primera herramienta que pueda estimar la misma en la etapa preliminar de diseño en colaboración con el astillero Chantiers de L'Atlantique.

Ya que las colisiones entre buques son consideradas como el estado accidental más peligroso, primero se destacan los intentos por la comunidad de investigación en estructuras navales por entender este suceso. Se revisa la literatura referida al análisis numérico de las colisiones de barcos para identificar los procedimientos actuales en la evaluación la resistencia estructural de objetos sujetos a cargas de impacto. Se presenta una relación entre los dichos métodos, así como también las limitaciones actuales en el campo de estudio de colisiones entre estructuras de buques. Se revela que aún se encuentran en bajo nivel de evaluación los requerimientos actuales de las Sociedades Clasificadores referidos a los problemas estructurales de colisiones de buques y varamiento.

En una siguiente etapa, se utilizó un reciente estudio de colisiones como base para la validación de un escenario de colisiones parametrizado utilizando LS-Dyna. La configuración del archivo de simulación es descrita considerando su relación con la subrutina MCOL para evaluar la dinámica externa de los buques considerados como cuerpos rígidos, donde finalmente se encontraron diferencias debido al criterio de falla de material asumido. Luego, considerando velocidad inicial en el barco golpeado se generaron colisiones no perpendiculares evaluando el daño perpetrado en base a la penetración en el costado y la energía interna disipada. Los mismos escenarios fueron reproducidos en el programa SHARP para después ser comparados y analizados. Se encontró que las formulaciones del programa SHARP limitan la contribución en la energía de deformación de diferentes componentes que de acuerdo con LS-Dyna, también se deforman. Además, se obtuvo que la energía debido a la fricción de componentes es más importante cuando se evalúan colisiones con ángulos agudos.

En una última sección, se propone una herramienta analítica basada en un diseño-compartido de energía para evaluar cargas de impacto en la etapa preliminar de diseño. La energía de deformación se obtiene en función del volumen de material afectado en ambos barcos que se asume igual a la energía cinética inicial del barco que choca. Se sugiere una velocidad límite para este barco estimada a partir de la máxima penetración permitida en el barco golpeado para evitar una explosión a larga escala. También, se generaron simulaciones con LS-Dyna para encontrar diferencias en el daño del barco, debido a un impacto a alta velocidad y a las formas de la proa del barco que impacta.

1. INTRODUCTION

1.1. Background and motivation

The safety of vessels in the trading industry is critical since it represents 90% of the worldwide trade economy and there are still many efforts to reduce it. Among the major risks considered to increase the losses of ships due to ship collisions are the busy seas, which are produced by the maritime traffic in some hotspots limited with geographically narrowed navigation spaces and by the constant increase of offshore wind-farm industry. By the year 2000, the reported number of total losses of ships over 100GT was around 207 according to (Allianz, 2019). Nevertheless, the implementation of regulations, advances in technology and improvement in ship designs have made this number decrease significantly up to less than 50 cases twenty years later. The main outcome would be this number to be null, but the risk of ship collision may still occur.

In the following 30 years, maritime congestion is expected to be increasing as predicted by (International Transport Forum, 2019). It has also been estimated that only passenger transport is projected to triple from 2015 to 2050 based on the current demand. Further, by following the constant growth in the offshore wind industry which has been explored mainly in Europe, the power capacity is expected to increase over 15 times in the next three decades, as reported by (Birol, 2019). Besides, challenges as human errors are responsible for 75% to 96% of the maritime accidents according to (Allianz, 2012) will also place the possibility of having a risk of ship collision. Therefore, even the minor of all these sources of eventualities may lead to great consequences as disruption of maritime traffic, losses of goods that could harm the environment and even in worst scenarios becoming into fatality cases. Then, the need to improve the ship designs to give the chance of mitigating major consequences under inevitable accidents is one of the strategies considered by the research community to reduce these numbers.

The overall safety of a ship is usually evaluated in terms of loss of stability as well as structural strength both assessed by deterministic and probabilistic approaches. In the common deterministic procedure, the actual structure is submitted to the corresponding load cases and rationally evaluated to verify its reliability. As the ship design progresses, more accurate procedures are required to be consistent with the evolution of the structural complexity of the ships. For the designers, it is worth having quick and easily applicable tools to initiate the

analysis in such a conservative way but also complex and very accurate procedures to finally approve the requirements of the classification societies.

The structural reliability of a ship hull exposed to external damage is partly focused on in terms of collision and grounding. These two types of accidental limits are highlighted when the design and analysis of fortuitous scenarios are performed so it is possible to evaluate the behaviour of the structure to resist such accidents. Collision analysis is nowadays studied through analytical formulations and numerical simulations. This latter may be examined with nonlinear solver codes such as LS-Dyna which applies the Finite Element Method for the nonlinear dynamics analysis of structures developed by Livermore Software Technology. The procedure involves the coupling between the internal mechanics concerned to the crushing of finite elements that are calculated by LS-Dyna considering a threshold for the failure of the material and the external dynamic effects coming from the global movements of the impacted structures performed by the included MCOL subroutine solving the hydrodynamic force equilibrium equations.

Analytical approaches as the one proposed by the super-element method have also been implemented on a friendly and quicker program called SHARP, developed by (Le Sourne, Nicolas, Cedric, & Natacha, 2012). In this approach, resistant forces and internal energies are calculated using the upper bound theorem but also coupled with external dynamics computed with MCOL code. It was found that although some improvements regarding simplifications that are heavily linked to the results of the SHARP program are required, it is worth considering this tool in terms of time and computation effort compared to the conventional non-linear FEM based numerical simulations.

In the framework of this study, non-right-angle collisions are also studied considering striking and struck ships with an initial velocity. To apply for the SHARP program as a formal design tool, it is worth discovering and recommending improvements to extend this range of applications. The large difference in the time required to generate a collision scenario using SHARP compared with any other Finite Element code lays foundations to use this approach in a preliminary ship design stage as soon as it is trustworthy. For this reason, this academic research was performed under the supervision of Professor Hervé Le Sourne (ICAM) authorized by the MAERM program from ETSI Navales (UPM) as the academic final dissertation of the ERASMUS MUNDUS program EMShip+ (3rd Cohort M120).

1.2. Objectives

Two goals are followed to fulfil the main purpose of this research about the understanding of the ship collision analyses:

- The main objective of this research is to develop numerical models to make comparisons of ship-ship collision scenarios. More realistic scenarios considering acute-angled impacts plus initial velocity for both striking and struck ships would extend the range of application for these kinds of analyses. Finite Element codes as LS-Dyna/MCOL may be able to generate such scenarios at the high computational effort as usual. On the other hand, the analytical tool SHARP has been evolving in the applicability of oblique ship collisions. Then, the goal in this section is to point out sources of discrepancies in time-penetration evolution and internal energy absorbed in the crushing process for both methodologies considering more acute collision angles.

- The second target is to implement an analytical approach for the study of the ship collision in the actual pre-design stage. It is important to establish a simplified approach to analyse the crashworthiness of a ship in an early design. Although the Finite Element Method is quite an accurate and trustable procedure, it is time-consuming. Design criteria as maximum penetration length or internal energy absorbed may be considered before generating complete ship collision models. This section aims to present to the industry an analytical methodology to estimate the crashworthiness of a ship in a simplified analytical way.

1.3. Methodology of the thesis

This research was structured in three main sections to fully integrate the concepts and the implementation of the proposal of the thesis. In the first section, a literature review regarding the ship-ship collision is performed. Then, following the first objective, simulations of ship collisions are executed with Ls-Dyna/MCOL and SHARP/MCOL solvers and discrepancies between results are analysed. And finally, a simplified analytical tool for the early ship design stage when considering crashworthiness analysis is presented. By the tracking of these three sections analysis of results, conclusions and recommendations are submitted.

In the section referred to Literature Review, an overview of the existing methodologies to assess the crashworthiness of structures is done. The importance of introducing the Accidental Limit States in the ship design is abstracted. Segregation of the different ship collision accidents related to offshore and side ships structures is mentioned. Some works of different authors lead to the use and relation between experimentation, analytical formulations, and numerical simulations. The two last being the most common due to their applicability but limitations in the prediction of the collision resistance are found in some cases. Finally, a link between LS-Dyna FEM code and MCOL for the understanding of the mechanics and dynamics for ship collision events is explained.

In the next section, the comparison between impact models using LS-Dyna and SHARP is carried out. Using a Benchmark collision study, it is validated a parametrized impact scenario using LS-Dyna. Comparison of penetration length and time-internal energy evolution aims to generate a model that will be able of producing results in some 'extreme' collision scenarios. Initial velocity in struck ship and collisions at acute angles will be set to produce such scenarios. Then, using the SHARP program, the same collision scenarios will be reproduced to compared results and find differences.

In section 4, it is proposed a quick pre-design analytical tool for the prediction of the crashworthiness of a ship in an early design stage. Analytical formulations were proposed by (Minorsky, 1958) for the study of large ship collisions and modified based on statistical and experimental observations to roughly predict the penetration length related to the volume of the crushed material. Numerical simulations are developed using LS-Dyna/MCOL codes to establish a first approach in the ship design relating the analytical formulation with some design criteria. All this section is developed in collaboration with the shipyard Chantiers de L'Atlantique to contribute to the implementation of future ship collision analyses.

2. LITERATURE REVIEW

The concern in the study of accidental scenarios has been introduced by the International Ship and Offshore Structure Congress (ISSC, 2018) in which collision, grounding, and explosion accidents are described with the state of art, pointing out to further research in such areas. The ship collision is defined as the major hazard among them and is classified according to the impacted structure. Some mention in the related investigations of this type of accident is developed in this section and feedback regarding the scope of this work is pointed out.

2.1. The accidental Limit States

The concept of Limit State Design is associated with the integral condition of an offshore structure which surpasses the design criteria it was built for. For analysis of structures, there are four different limit states to be considered: Serviceability Limit State (SLS), Ultimate Limit State (ULS), Fatigue Limit State (FLS) and Accidental Limit State (ALS). The latter is dedicated to the identification of accidental loads and nonlinear structural consequences in ships and offshore structures as published by (ISSC, 2018).

Among the most common accidental scenarios, ship grounding and collisions are considered hazard events with a high risk of failure. In the study and design of complex structures, experimentation is rarely suggested due to restrictions of full-scale models but procedures to create a rational analysis may be applied regarding the design situation as shown in Figure 2.1. In many cases, accurate modelled FEA becomes the most powerful tool for assessing ALS criteria. One common result in the evaluation of the crashworthiness of a structure is the absorbed internal energy. This can be obtained using FEM up to certain failure criteria or also using analytical or empirical formulations.
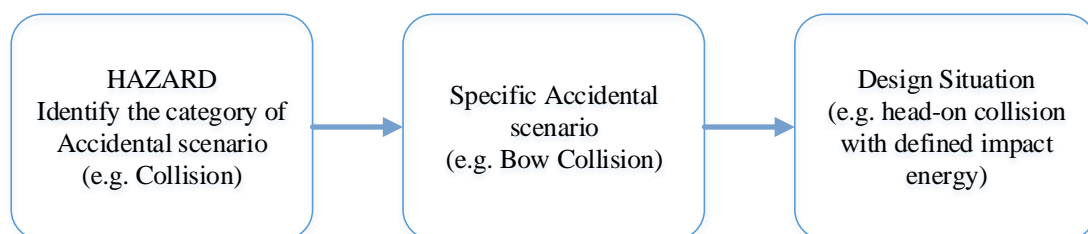

Figure 2.1. Flowchart for the definition of design situation in ALS.

Source: (ISSC, 2018)

2.2. Ship-Ship collision studies

When collision accidents are considered for the ship design, the aim is either to avoid the event or to ensure the condition of navigation after the impact. In the latter, the ship safety may be evaluated in terms of loss of stability due to the flooding of the compartments and reliability of the structure when damaged. Researchers are promoting methodologies for the prediction and analysis of structures at rest impacted by ships. Analytical and numerical tools are supporting the investigation of such events that are expected to be accepted by the marine engineering scientific community to prevent several losses as environmental pollution or even fatalities.

The pioneer in the development of simplified formulas was (Minorsky, 1958) who found a relation between the energy absorbed by a struck ship and the volume of damaged steel. He established an empiric formulation based on a set of 27 experiments, rather easy to apply mainly for large scale energy collisions although no influence of the surrounding water on the ship dynamics was included. Some improvements in these empiric energetic methods were far after proposed by (Perdesen & Zhang, 1998), who considered three modes of energy absorption in the collision: plastic deformation by membrane tension, folding and cutting of plates. More details about the material characteristics and dimensions can be found in their formulations, however, only the internal mechanics of plates deformation is analysed in the collision. (Lehman & Peschmann, 2002) used the results of large-scale collisions experiments to validate numerical calculations. Great efforts were given by more authors to assess the crashworthiness of structures, nonetheless, in most of the cases full-scale experimentation was needed, but limitations are found due to the expensive production of the tests.

The use of computational tools boosted the analysis of ship crashworthiness applied with numerical methods but more details in the modelling procedure are in demand. Numerical simulations have been performed for the analysis of lock gates impacted by river ships as presented by (Le Sourne, Rodet, & Clanet, 2002). The influence of the external dynamics for the interaction of the hydrodynamics effects over an impacted structure has been simulated with a rigid body large rotational formulation by (Le Sourne, Donner, Besnier, & Ferry, 2001). Based on experimental observation, (Simonsen & Lauridsen, 2000) presented the prediction of plate failure for the analytical and finite element calculations. A failure criteria benchmark study based on right-angle collisions simulations were performed by (Ehlers, Broekhuijsen, Alsos, Biehl, & Tabri, 2008), to determine the force-penetration curves disregarding the external dynamics.

The need for rapid estimations for the collision analysis is convenient when numeric simulations and experimentation need baselines for their setup. (Zhang, 1999) proposed formal mathematical models for the collision energy losses, collision forces and structural damage, considering the interaction of external dynamics as part of the analysis. One of the first rapid approaches was given by (Lützen, Simonsen, & Pedersen, 2000), in which mathematical models to predict the damage on both side structure of a struck vessel and an idealized striking bow are given. The prediction of the internal mechanics of the struck ship follows the so-called super element method. (Le Sourne, Besnard, Cheylan, & Buannic, 2012) implemented the approach in a user-friendly program, which calculates the internal forces and energy of the impacted elements following the upper-bound theorem. At each indentation step, the calculated forces are transmitted to an external dynamic program for the hydrodynamic equilibrium equations to be solved. While performing quick simulations, a good performance for perpendicular ship collision was obtained from the program, but some improvements for large-angle oblique collisions were added.

Benchmark studies are baselines for the development and validation of analytical and numerical tools. In a recent work developed by (Le Sourne & al., 2021), two benchmark studies are presented in which the analysis of ship collision and ship grounding are simulated with both explicit nonlinear finite element and super-element methods. Approaches that were used with the computational tools LS-Dyna and SHARP program respectively. The ship collision simulations are based on a struck ship at rest impacted at its midship section with two different orientations of the striking ship. Some simulations were generated as a perpendicular impact at different longitudinal locations of the struck ship. An additional scenario was considered with an impact orientation of 45 [deg.] regarding the surge direction of the struck ship.

(Liu, Pedersen, Zhu, & Shengming, 2018) recently show the importance of large-scale collision experiments to explain the challenges in the full evaluation of the crashworthiness of ship structures using analytical and numerical procedures. As shown in Figure 2.2, there is an important relation among the existing procedures for the analysis of structural failures subjected to impact loads. In this study was found there is a lack of knowledge about the collision of a deformable striking bow and the side structure of a ship. Besides the estimation of the energy dissipated by friction during the collision is still a topic under research and implies the need for future improvements. It was found that classification societies are still at a primitive level regarding the assessment of damage extent due to collision and grounding of ships.

```
┌─────────────────────────────────────────────────────────┐
│        Impact strength of ship structural components      │
└─────────────────────────────────────────────────────────┘
```

Numerical simulation	**Experiment**	**Analytical method**

| Definition of material nonlinearities | Tensile test | Failure modes of structural elements |

| True stress-strain curve | Fracture Strain | Analytical formulae |

| Simulations of large-scale structures | Experiments of large-scale structures | Structural energy absorptions |

Verification   Verification

```
┌─────────────────────────────────────────────────────────┐
│              Analysis of structural failures              │
└─────────────────────────────────────────────────────────┘
```
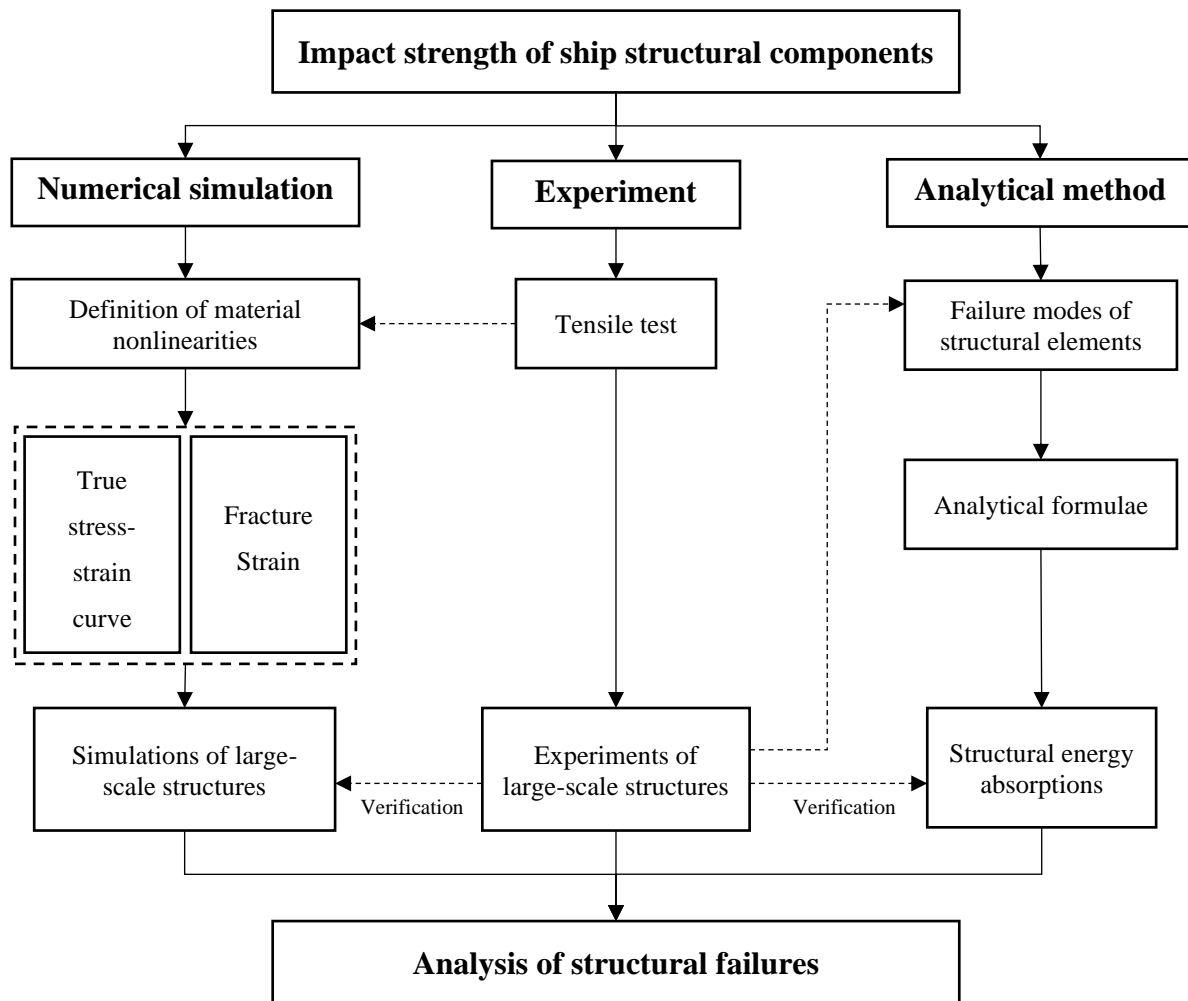
Figure 2.2. Relation of the methodologies for the analysis of impact strength

Source: (Liu, Pedersen, Zhu, & Shengming, 2018)

Inland navigation collisions were investigated by (Sone Oo, 2017) in the framework of the European regulation for the carriage of dangerous goods. It was found that environmental inland conditions for the navigation of vessels locate the ships at similar impact height, deforming plates from bottom and deck simultaneously. It results in some contribution to the deformation energy from the elements that are not physically impacted but interact in the crushing process. The super-element-based method relies on the independent interaction of the elements affected while the penetration increase.

In the contemporary research review, the prediction of plastic response of structures subjected to external impact has been accurately predicted for right-angle collision impacts. Analytical and numerical approaches prove to have good correspondence with the study of striking ships impacting even with some small inclinations from the perpendicular orientation. The impacted structure makes the difference in the categorization of the type of ship collision, which has been mentioned as offshore structures, lock gates and side ship structures. By the nature of these

considered deformable structures, are expected to be at rest but in case of not fixed structures as ship-ship at rest or ship-semi submersible turbine collisions, a global dynamics interaction is likely to happen after the impact. Some initial velocity in the case of ship-ship collision can demand an additional effort for analysis. More parameters in energy dissipation as the frictional energy produced from sliding of surfaces may contribute to the crashworthiness prediction.

2.3. Theory of numerical simulations for ship collision

The structural damage of collisions began to be studied with the impact between ships and submarines aided with the finite element method. The phenomena can be studied numerically by considering the interaction between mechanical deformation and external hydrodynamic loads. The subdivision of the crushing problem was proposed by (Pedersen, 1995) and (Petersen, 1982), and is nowadays accepted for the numerical assessment of the ship collision analyses.

2.3.1. Coupling between internal mechanics and external dynamics

In the internal mechanics, a nonlinear finite element calculation is managed to calculate the problem of buckling, yielding and rupture of the materials due to the collision of the structures. Subsequently, the hydrodynamic loads over the structures are computed with the MCOL code, assuming the global movement of rigid bodies, see Figure 2.3.

To make the calculation less costly in terms of computational time and relate the interaction of external global motions, the ships are embodied by a meshing of the zone of interest to be deformable plus a rigid one to represent the remaining part of the ship but also to recover the hydrodynamic information, (Le Sourne & al, 2003). With the FEM meshes, the solution of all the internal forces is obtained by the contact interaction in the crushing process. Then, the forces are transmitted to MCOL which uses information of hydrostatic restoring matrix, added mass matrix and the frequency-dependent added damping matrices of each ship to compute and returning nodal positions, velocities, and accelerations for the next iteration.
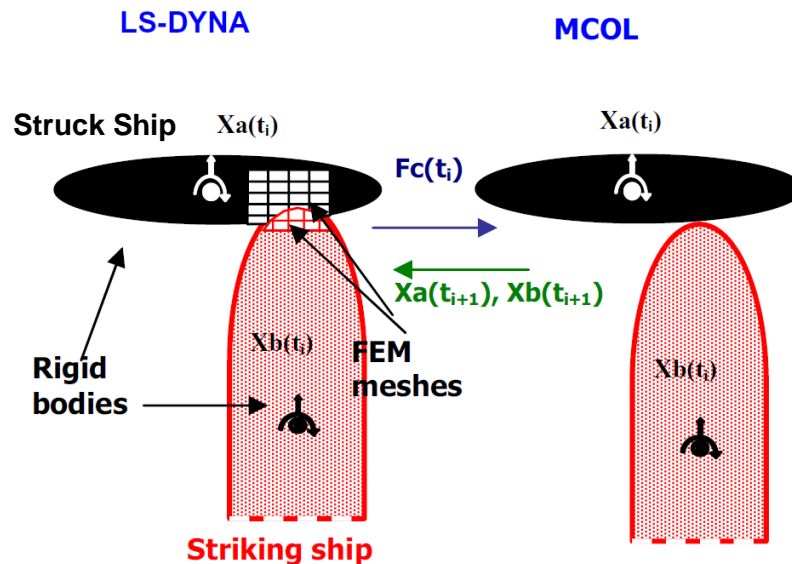
Figure 2.3. Global collision scenario simulation

Source: (Le Sourne & al, 2003)

The hydrostatic properties of the ships can be computed by any 3D sea keeping code and implemented in a text file to then be called at each iteration.

2.4. LS-Dyna FEM coupled with MCOL program

Finite element codes like Ls-Dyna have become the most powerful tools for the study of nonlinear dynamic events. In contrast with implicit calculation, LS-Dyna allows predicting the time-evolution for large time-dependent deflections in quite small periods with no need for a global system of equations to enforce the equilibrium by an iterative process. Effects as shock wave propagation are possible to be capture due to the smaller but inexpensive time steps required making the solution also conditionally stable. Nonetheless, for both cases in the numeric calculation, it is demanded to solve the following discrete equation of motion:

$$[M]\{\ddot{u}(t)\} + [C]\{\dot{u}(t)\} + [K]\{u(t)\} = \{F(t)\}$$

Eq. 1

Where the right term $\{F(t)\}$ represents any external load applied on the system while the sum of the left terms aims to find the equilibrium to such load. In the latter, $[M]$ is the structural mass matrix, $[C]$ is the damping matrix and $[K]$ the stiffness matrix. In addition, nodal displacements, velocities, and accelerations are contained in $\{u(t)\}, \{\dot{u}(t)\}$ and $\{\ddot{u}(t)\}$ respectively.

The direct integration scheme adapted to solved Eq. 1 is the Newmark Method. Then a prediction of the acceleration is obtained by solving Eq. 2, Eq. 3 and Eq. 4 if the solution depends only on the acceleration of the previous step, $\ddot{u}_n$. For this reason, it is mandatory to set

initials conditions in the system, for instance, $u(0) = u_0$ and $\dot{u}(0) = \dot{u}_0$. The solution is finally predicted by the following set of equations:

$$M\ddot{u}_{n+1} + C\dot{u}_{n+1} + Ku_{n+1} = F_{n+1} \qquad \text{Eq. 2}$$

$$u_{n+1} = u_n + \Delta t\, \dot{u}_n + \frac{\Delta t^2}{2}[(1 - 2\beta)\ddot{u}_n + 2\beta\ddot{u}_{n+1}] \qquad \text{Eq. 3}$$

$$\dot{u}_{n+1} = \dot{u}_n + \Delta t\,[(1 - \gamma)\ddot{u}_n + \gamma\ddot{u}_{n+1}] \qquad \text{Eq. 4}$$

In Eq. 2, F_{n+1} is the vector of all the external loads at the time t_{n+1}. Besides, the system is decoupled when the matrix $[M]$ is diagonal. The method is said to be computationally efficient in exchange for unconditional stability when converging to the solution. It must be guaranteed that all the effects in the impact are being captured by the explicit solution. The maximum time step defined in Eq. 5 should be smaller than the time taken by shock wave to go through a finite element at the velocity of the sound in that material and it is usually in the order of micro secs.

$$\Delta t \leq min\left(\frac{1}{c}\Delta x^{element}\right) \qquad \text{Eq. 5}$$

The value of c in Eq. 5 is defined according to the type of the finite element, for instance:

$$c = \sqrt{\frac{E}{\rho}} \qquad\qquad\qquad c = \sqrt{\frac{E}{\rho(1 - v^2)}}$$

For bar elements   For shell elements

2.4.1. Rupture criteria

The rupture criteria of the material are defined as a threshold of the strain calculated in the elements of the model. For shell elements, this can be referred to as the strain computed through the thickness of the material. All the overstrained elements are removed from the calculation and do not contribute any longer to the deformation energy of the solution. This value is set up manually by the user to give a realistic representation of the phenomena. About the numerical analysis, the failure of the material must be defined from experimentation as defined in Figure 2.2. (Lehman & Peschmann, 2002) proposed the most common formulation for the definition of the failure strain based on experimentation and is given by Eq. 6. When there is a major influence from the ratio between the thickness and the element length a constant value of 0.2 for the failure strain may be considered as mentioned by (Simonsen & Lauridsen, 2000).

$$\varepsilon_f(l_e) = \varepsilon_g + \varepsilon_e \frac{t}{l_e}$$

Eq. 6

(Umunnakwe, 2020) developed an extensive review and sensitive analysis around the definition of the strain failure for numerical analysis. A benchmark analysis was performed and the differences in the formulations to estimate the failure strain are mentioned about the prediction of the material failure in ship grounding simulations.

2.4.2. MCOL program

When collision forces are computed at each step, these are transferred to the implemented code MCOL for the computation of the hydrodynamic forces. The global ship motions are considered as the large dynamic rotation of two rigid bodies subjected to collision forces. The dynamic equations of motion are split into translational and rotational motion, to describe the 6 degrees of freedom.
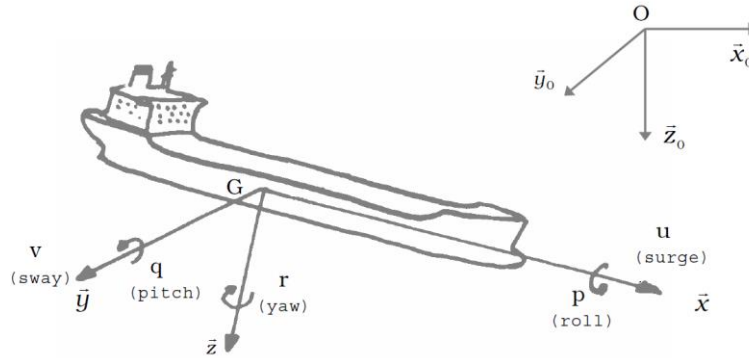
Figure 2.4. Body-fixed, earth fixed frame of reference.

Source: MCOL – Theoretical manual (Principia Marine)

The motions are described by Eulerian angle representation as defined by Eq. 7, Eq. 8 and Eq. 9 which are based on the actual frame of reference of the ship, see Figure 2.4. The vector x defines the earth-fixed position of the center of mass of the ship, y the body-fixed components of the linear and angular velocity of the centre of mass, v and ω respectively. The forces and moments of the body-fixed components are described with the vector f.

$$x = (x_{0G}, y_{0G}, z_{0G}, \phi, \theta, \psi)^T$$

Eq. 7

$$y = (u, v, w, p, q, r)^T = (v^T, \omega^T)^T$$

Eq. 8

$$f = (X, Y, Z, K, M, N)^T$$

Eq. 9

The free rotation of a body in the space involves the description of the rigid body representation as explained by (Le Sourne, Donner, Besnier, & Ferry, 2001). Rotation matrices are required for the transformation from body-fixed to earth-fixed frame components. Once this is achieved, Newton's law is used to define the rigid body motion concerning the body fixed rotation. The definition of added masses, restoring forces, viscous forces and wave forces are required for the definition of the hydrodynamic forces and moments because of the surrounding fluid. The equation of motion can be fully described considering the contact forces F_C which is part of the collision action.

$$M\dot{y} + Gy = [F_w + F_H + F_V](y, x) + F_C$$

<div align="right">Eq. 10</div>

The total mass of the body M, is defined by the mass of the rigid body plus the water added mass and G is the gyroscopic matrix. Due to the complexity in the integration of Eq. 10, a sub-cycling technique is introduced, in which the hydrodynamic forces of the equation are updated with a different time-step than MCOL calling frequency. Forces remain constant every two evaluations while there is an internal computation for new expressions for position, velocities, and accelerations.

2.5. SHARP program

In the aim of having a quick prediction of the structural damage induced by the collision of ships, a super-element-based program was implemented on user-friendly software by (Le Sourne, Besnard, Cheylan, & Buannic, 2012). The mathematics behind the program is based on the upper bound theorem, applied to calculate the internal resistance forces and energies of structures subjected to large and sudden external forces. Global dynamics motions are calculated with the MCOL program as shown in the previous section, after the transmission of the crushing forces due to the collision. Total internal energy deformation and penetration length in the struck ship may be obtained and a good estimation of the damage has been demonstrated for perpendicular and large angle oblique collision impacts. The versatility of the interface allows for the easy variation of the parameters of the collision such as longitudinal and vertical impact locations, angle of impact and initial velocity in the struck ship.

2.5.1. Definition of the upper bound theory

The design of a beam is based on the definition of its carrying capacity and its plastic collapse is reached when an external load overpasses this capacity limit. (Jones, 1990), proposed a plastic collapse theorem for beams called the upper bound theorem valid for the calculation of the exact collapse load of a system. This postulate that '*if the work rate of a system of applied loads during any kinematically admissible collapse of a beam is equated to the corresponding internal energy dissipation rate, then that system of loads will cause collapse, or incipient collapse, of the structure*'. It is expected for a mechanism to be considered as kinematically admissible, if its displacement field satisfies the displacement boundary conditions, constant volume (plastic incompressibility) and only positive work due to external loads. Applying this theorem in a simple example for the calculation of static plastic collapse of a cantilever beam loaded in the end, the transverse velocity field on this beam is considered as depicted in Figure 2.5b.
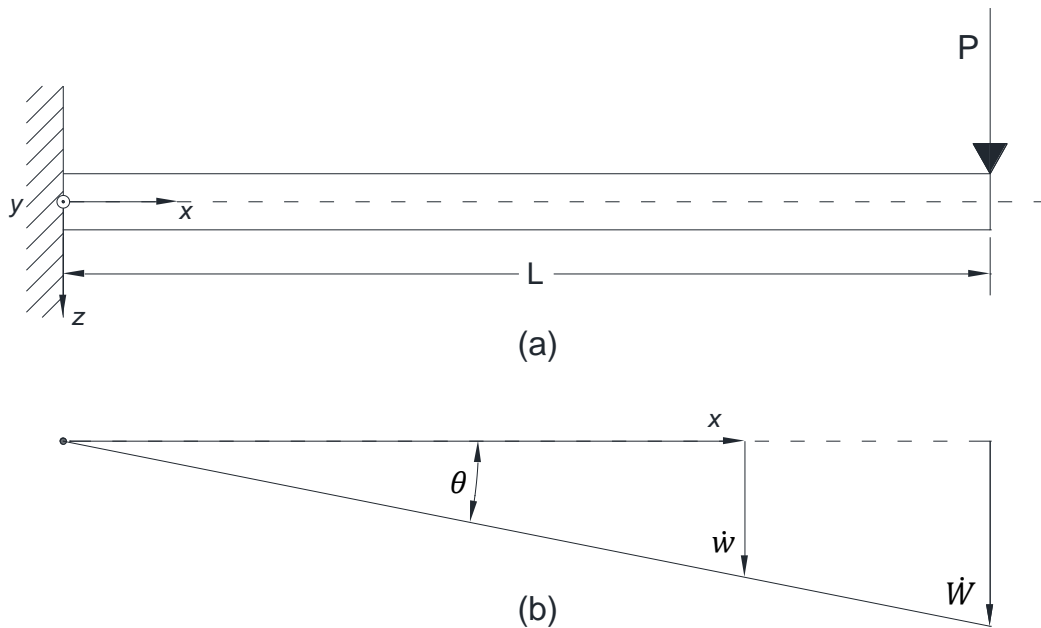

Figure 2.5. Beam in cantilever. (a) External load in the end (b) Transverse velocity profile

Source: Book, Structural impact. (Jones, 1990)

The upper bound theorem states that:

$$M_0 \dot{\theta} = P^u L \dot{\theta}$$

Eq. 11

Then the exact collapse load of the beam is defined as:

$$P^u = \frac{M_0}{L}$$

Eq. 12

In general terms, the application of this theorem is reduced to the evaluation of the external and internal energy rates of a discretised system of super-elements, as presented in Eq. 13 and Eq. 14 respectively. The external energy is the one dissipated by the crushed super-element, it can be evaluated with the estimation of the resistance force F while indentation δ in the struck ship increases. While the internal energy of a solid body is obtained with the relation of the stress and strain rate tensor.

$$\dot{E}_{ext} = F \cdot \dot{\delta}$$

Eq. 13

$$\dot{E}_{int} = \iiint_V \sigma_{ij} \cdot \dot{\varepsilon}_{ij} \cdot dV$$

Eq. 14

Close-form expressions for the evaluation of the collision resistance are obtained by considering some assumptions, especially for the arduous task in the calculation of the internal energy rate. To simplify the theoretical calculations, the moment-curvature relation is often replaced by a perfectly plastic or bilinear approximation. This is done by defining a flow stress, which is usually calculated as the mean value between the static yield stress and the ultimate stress. The internal energy contribution is firstly given by bending deformation because of a certain number of plastic hinges and a second one due to a membrane effect of plates.

2.5.2. Super-element definition

The side structure of the struck ship is represented by a set of macro-elements assumed to deform in a plastic domain when they receive a perpendicular impact. The individual contribution of the resistance of each super element upon the striking rigid ship will define the total internal energy. For the case of perpendicular collision impacts, super-elements may be discretised into a set of four types of elements according to (Lützen, Simonsen, & Pedersen, 2000), which are the most common when using this approach. Large plates, such as side shells, or longitudinal bulkheads, will follow the deformation patterns of Figure 2.6a. Inner decks and bottom plates are assumed to deform with an in-plane load as Figure 2.6b assuming clamped edges. The stiffening system and intersection of plates may be laterally loaded as shown in Figure 2.6 (c,d).

(a) Plate subjected to punctual lateral load   (b) Plate folding after inplane load in one edge

(c) Beam subjected to punctual lateral load   (d) Plate folding after inplane load in one edge
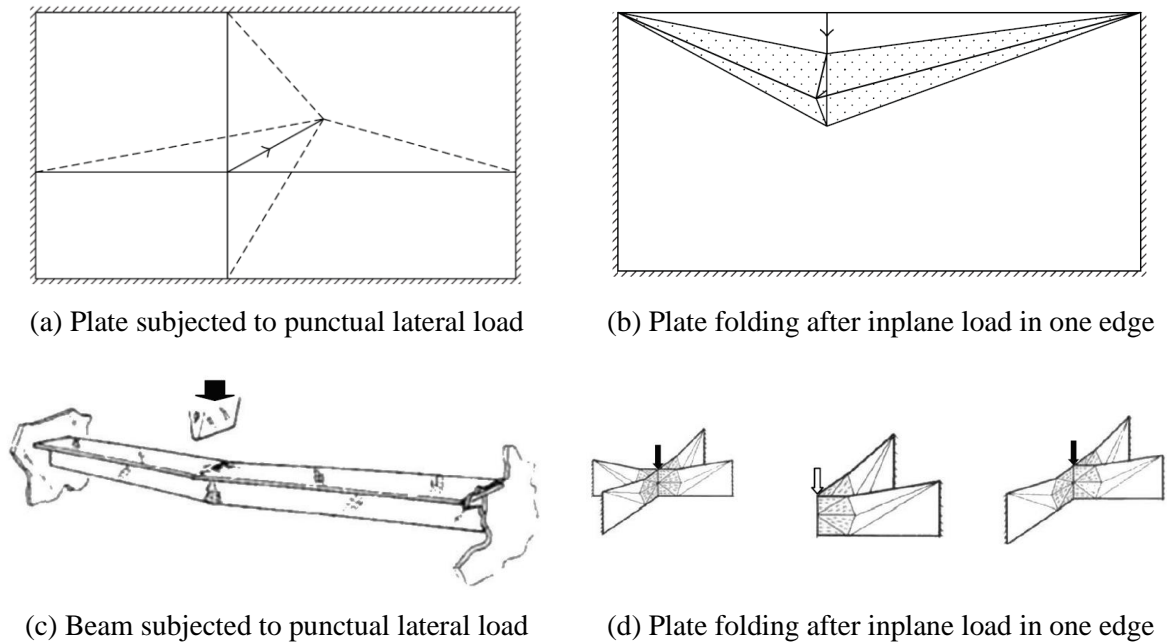
Figure 2.6. Basic super-element derivation for right-angle collision impacts

Source: (Le Sourne, Besnard, Cheylan, & Buannic, 2012)

Closed-form expressions are derived from the plastic mechanism behaviour of each super-element. At each indentation step, the total internal energy is calculated with the contribution of all the super-elements. (Le Sourne, Donner, Besnier, & Ferry, 2001) added a generalization for oblique collisions cases by including six different super-elements. A typical structure arrangement of a ship can be well represented with the use of this methodology to quickly assess the damage of a collision impact between two ships.

3. FRAMEWORK AND VALIDATION OF THE IMPACT MODEL USING FEM AND SUPER-ELEMENT METHOD.

A comparison of two methodologies to analyse the collision between two ships both with initial velocities is developed in this section. By considering parameters as initial velocity in the struck ship and acute-angled collisions, some 'extreme' scenarios are tested to evaluate the limitations of numerical and analytical approaches considered by LS-Dyna and SHARP respectively. In the case of LS-Dyna, collision scenarios are performed using a parametrized file that is validated firstly by comparing its results using a Benchmark collision study. Then in a second stage, the collision parameters are recreated in the SHARP program to obtain results and then be compared.

3.1. Benchmark collision study

The use of numerical simulations to assess the damage due to collision and grounding justifies the importance of reducing uncertainties in the modelling process. (Le Sourne & al., 2021) presented a comparison of several ship collision simulations performed by four participants using non-linear explicit FEA and super-element method to assess numerically the damage caused by ship-ship collision and ship grounding. Each participant used different computational tools to simulate the structural mechanics and global hydrodynamics, these are summarized in Table 3.1.

Table 3.1. Software used by the participants of the paper

	Participant	Hydrodynamic Simulation	Structural Analysis
Collision	AALTO	In-house Code	LS-Dyna / MCOL
	ICAM	Hydrostar	SHARP / MCOL
	MARIN	MARIN XMF	MarcolXMF
	MSRC	Ansys AQWA	LS-Dyna/MCOL

Source: (Le Sourne & al., 2021)

Three right-angle and one inclined collision scenarios were simulated and compared using the same target ship structures. A cruise ship (Ship A) was considered as the Struck Ship, which is impacted at two different locations around midship section while being at rest ($V_{0,A} = 0$). The first location is referred to as a 90 degrees (between ship surge directions) collision on the transversal bulkhead which is located at 95.5 m from F.P. as shown in Figure 3.1.

The second location is set at 103.95 m from F.P. and two collision orientations are considered in this zone: also, one considering 90 degrees and a second of 45 degrees (both referenced to the surge direction of the striking ship).
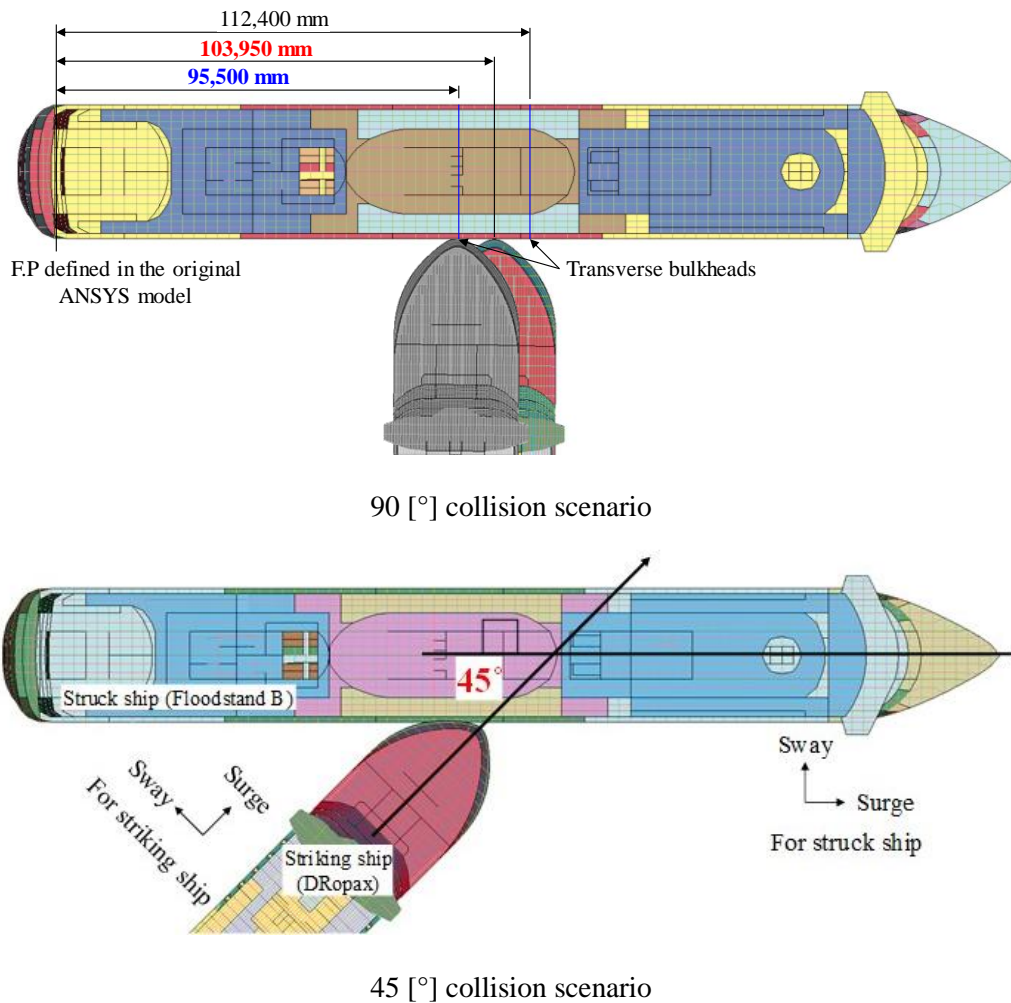
90 [°] collision scenario

45 [°] collision scenario

Figure 3.1. Description of the collision scenarios.

Source: (Le Sourne & al., 2021)

The striking ship (Ship B) is represented by a RoPax that is impacting in three scenarios at 5 knots and one at 10 knots. Finally, all the collision scenarios considering only variations in the impact location and initial velocity of the striking ship were arranged as follows:

Table 3.2. Striking Ship collision scenarios

Scenario	Velocity	Angle	Location
	[knots]	[°]	from F.P. [m]
1	5	90	103.95
2	10	90	103.95
3	5	45	103.95
4	5	90	95.5

The time evolutions of internal energy and penetration length were the common criteria for all the participants to compare their results. At the same time, the internal energy is accounted for the contribution of the deformation energy and the one dissipated due to the friction of the elements in contact. Since the super-element method was developed from closed-form expressions to calculate the resistance of the structural elements there is no differentiation of the effect of plastic deformation and frictional dissipation in the SHARP program, being this a point to consider later for the analysis. Figure 3.2 summarizes the structural response of the collision scenarios in terms of maximum penetration and maximum internal energy dissipated.
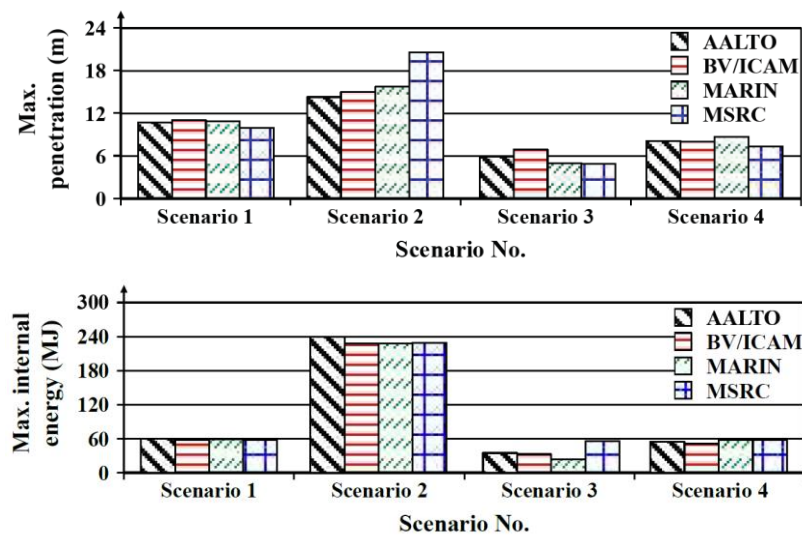

Figure 3.2. Maximum structural response of the collision study

Source: (Le Sourne & al., 2021)

The good accordance between the maximum results obtained in the collision benchmark study validates the agreement between both methodologies to estimate the crashworthiness of perpendicular ship collisions. Some recommendations in the modelling process were found for the finite element method when frictional energies seemed to be sensitive to contact definitions. Besides, some differences in the super-element-based approaches for scenario 3 (oblique impact) are noticed. Lower values for penetration and internal energy in MARIN's approach were obtained since there were still under verification of the horizontal in-plane collision elements. Meanwhile, for same scenario 3, BV/ICAM seems to have better results with their SHARP program. The oblique collision is fitting closer with the finite element calculations. The results presented in the collision benchmark study will be used to validate a parametrized collision scenario in a further stage.

3.2. Set-up of a Non-Linear Finite Element Model in LS-Dyna/MCOL.

The generation of a collision scenario is based on a set of keyword inputs that are logically organized so that LS-Dyna can simply understand and execute. Each keyword is written in a text file with extension ***. k** and sharing similarities depending on the role of the text file in the collision scenario. To represent the physical behaviour of an impacted offshore structure, mechanical and hydrostatic properties must be properly represented with two specific text files, as shown in Figure 3.3. For instance, the mechanical deformation of the struck ship is represented by a set of nodes and elements listed in rows and columns using the keywords *NODE and *ELEMENT and all storage in a ***. k** file. The global external dynamics of the struck ship is predicted by given hydrodynamic properties (water added mass, hydrostatic restoring and wave radiation damping) stored in a text file with the extension ***.mco**. The same information for the striking ship is required by the main file with extension ***. k** containing additional keywords that will govern the parameters of the collision scenario. At the end of the simulation, a group of results are obtained according to the information requested by the user.
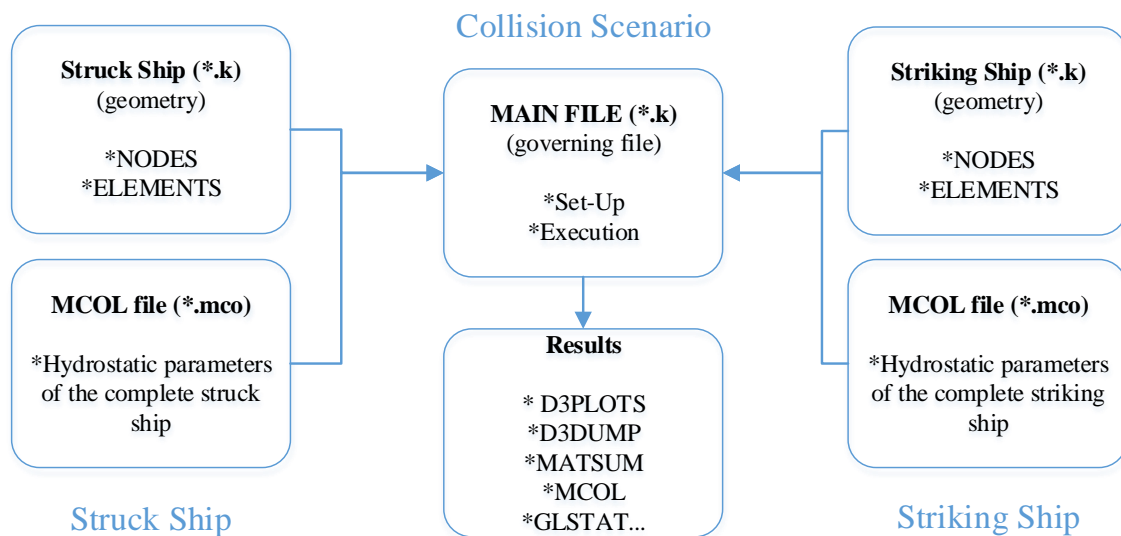

Figure 3.3. Organization chart for a collision scenario using LS-Dyna

Several simulations are run to validate the collision model regarding the Benchmark study without considering Scenario 2 since its high initial kinetic energy is out of the scope of the study. The same mesh of the ships used in this study is generated separately also with the hydrostatic parameters presented in the following section.

3.2.1. Description of the struck and striking ship models.

The collision scenario is based on a deformable struck mesh impacted around its midship section by a rigid bow shape of a RoPax as presented in Figure 3.1. The mesh of the struck ship represents a half beam section of the real ship equal to 16.1 [m], 72.8 [m] length and 15.94 [m] height. With a constant transverse section, six transverse bulkheads are distributed along with the model, also side shell, bottom shell, and main deck. Besides, horizontal structures were defined such as double bottom and three intermediate decks. Different colours in Figure 3.4 graphically represents that such elements are associated with a specific family of elements, named Parts. All the elements grouped in one part will share similar properties such as material properties, thickness for shell elements and dimensions or resultant modulus for beams elements.

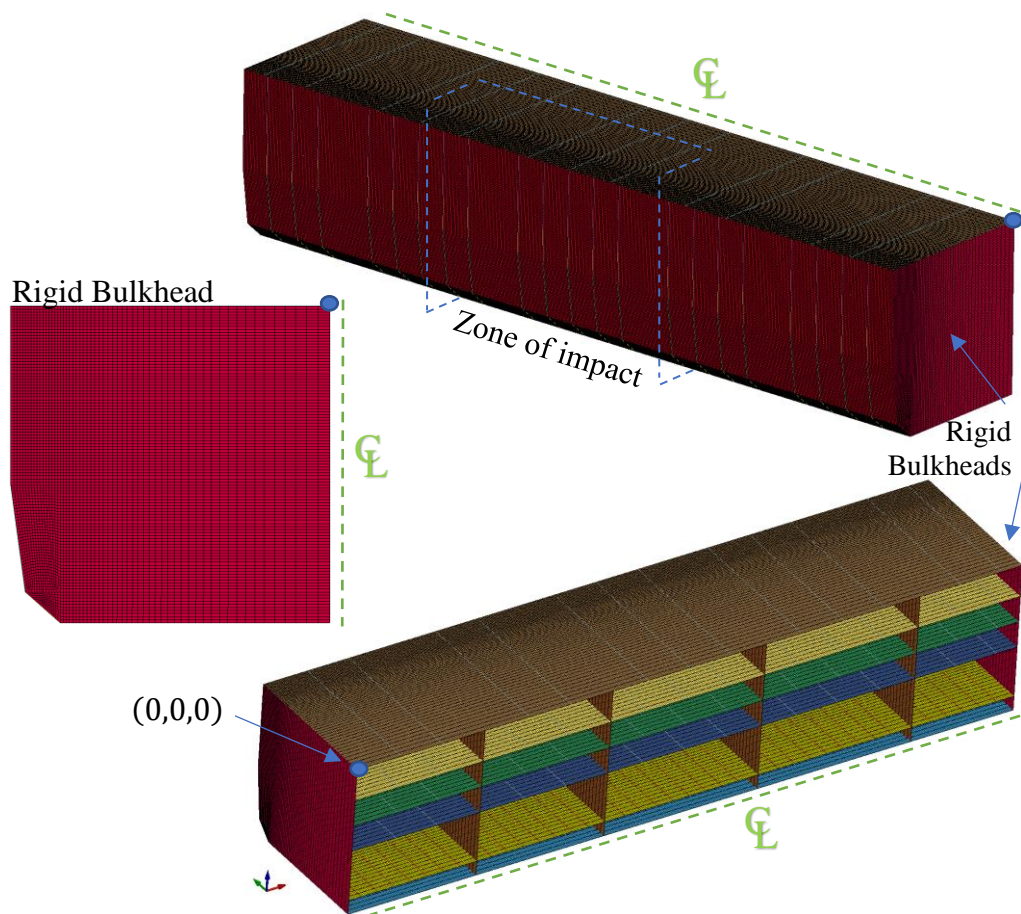Figure 3.4. Description of the Struck Ship model

The average mesh size of the model presented in Figure 3.4 is 150 [mm] mainly around the zone of impact. It contains a total of 307761 nodes and 315362 elements between shells and beams each defined in between groups of four and two nodes respectively. Only the beams expected to deform in compression in the direction of the side impact were modelled. The two

extreme farthest bulkheads from the impact zone are treated as rigid bodies associated with the remaining inertia properties of the complete ship and for transferring the global response determined by the MCOL solver.

The mesh of the striking ship is not deforming in the crushing process since it is considered as a rigid part of 45 [m] length from forward, see Figure 3.5. The inertia properties of the complete ship are directly associated with this part that is also containing the hydrostatic parameters required by MCOL. Since this mesh is not participating in the internal mechanics' calculation, LS-Dyna will not consider these elements for the time step calculation. Good quality mesh is not required when rigid bodies are defined, however, the striking ship mesh size should be similar to the one used for the struck ship to avoid contact detection problems. An average mesh size of 200 [m] for the striking elements is used although are considered rigid.
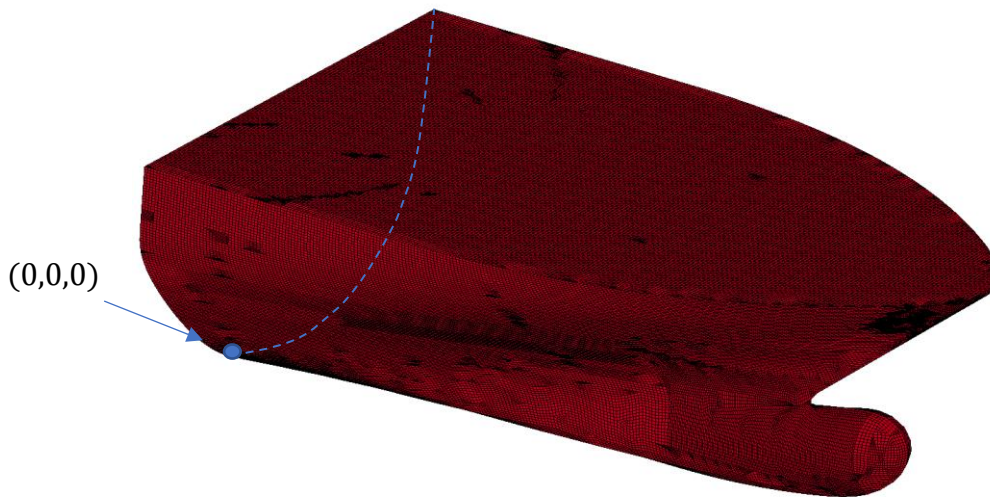

(0,0,0)

Figure 3.5. Description of the Striking Ship model

3.2.2. Parametrized collision scenario

A third ***. k** file is required to govern the main parameters and execute the impact between the two models. In this file is described a group of keywords that define properties such as, real simulation time, materials characteristic definition, the behaviour of contact interface, the association of global inertias with rigid parts, link-up with MCOL boundaries, initial conditions, and so on. The details about the definition of the keywords required for the setup of the collision scenario are described in APPENDIX A1.

A parametrization of the initial conditions is managed at the top of the file to easily generate variations in the impact collision scenario. As with many programming codes, a family of variables may be defined at the beginning to quickly change all the numerical values related to

these expressions and are named parameters. The keyword *PARAMETER allows to allocate numerical values inside alphanumeric parameters that start with the letter R and later be used in another data block, for instance, Figure 3.6 shows all the parameters defined for the striking ship. Since the struck ship is considered at rest, the validation is made giving a certain velocity in the striking one. Initial velocity, angle of impact and position are parametrized. Further parametrization is done to manage the initial conditions of the struck ship.

```
*PARAMETER
$                           For stricking ship _ SHIP B
$==============================================================================
$                                        Deck bow point at 45.179m from Ref.
$   Veloc_knots   |    angle_horizt   |   X_Position (m)  |    Y_Position (m)  |
$    PRMR1|     VAL1|    PRMR2|     VAL2|    PRMR3|     VAL3|    PRMR4|     VAL4|
RVELOCIT_B       5.0 RANGLE_H       90.0 RX_TRASL       35.6 RY_TRASL       61.34
$  Y_Position (m)  |    Z_CoGravity   |
$        |        |        |        |
  RZ_TRASL    -15.64     RZG_B    -2.115
```

Figure 3.6. Initial conditions of the striking ship

A post-treatment of the parameters is required in some cases to properly fit with the global frame of reference of the collision scenario. To be unit consistent in the setting up of the collision scenario, all the numeric expressions of these simulations are set in [m], [kg] and [sec]. The keyword *PARAMETER_EXPRESSION allows performing algebraical operations when needed. For instance, Figure 3.7 shows the internal conversion from [knots] to [m/s] of the surge velocity of the striking ship. Later, this parameter can be used after typing the symbol '&', i.e., &VELB.

```
$                                   conversion of velocity to m/s
*PARAMETER_EXPRESSION
$   PRMR1|     VAL1|
RVELB      (VELOCIT_B)*0.5144
```

Figure 3.7. Conversion of the velocity of the striking ship

By modifying the parameters set up in the top part of the collision file as shown in Figure 3.6, all the collision scenarios are easily generated. Several simulations modifying impact position, angle of impact and velocity of the striking ship are run to fit with the results of the benchmark study.

3.3. Definition of the collision scenarios for validation of the model.

Three collision scenarios from the benchmark study were used to validate the parametrized collision file. From a top view, Figure 3.8 shows the collision scenarios at different angles and longitudinal positions of the struck ship. For scenarios 1 and 3, the struck ship is considered at rest and is being impacted with a velocity of 5 knots between two bulkheads located at 95.5 [m] and 112.4 [m] from F.P. as defined in Figure 3.1. In Scenario 4, the striking ship impacts the bulkhead located at 112.4 [m] with the same initial velocity.
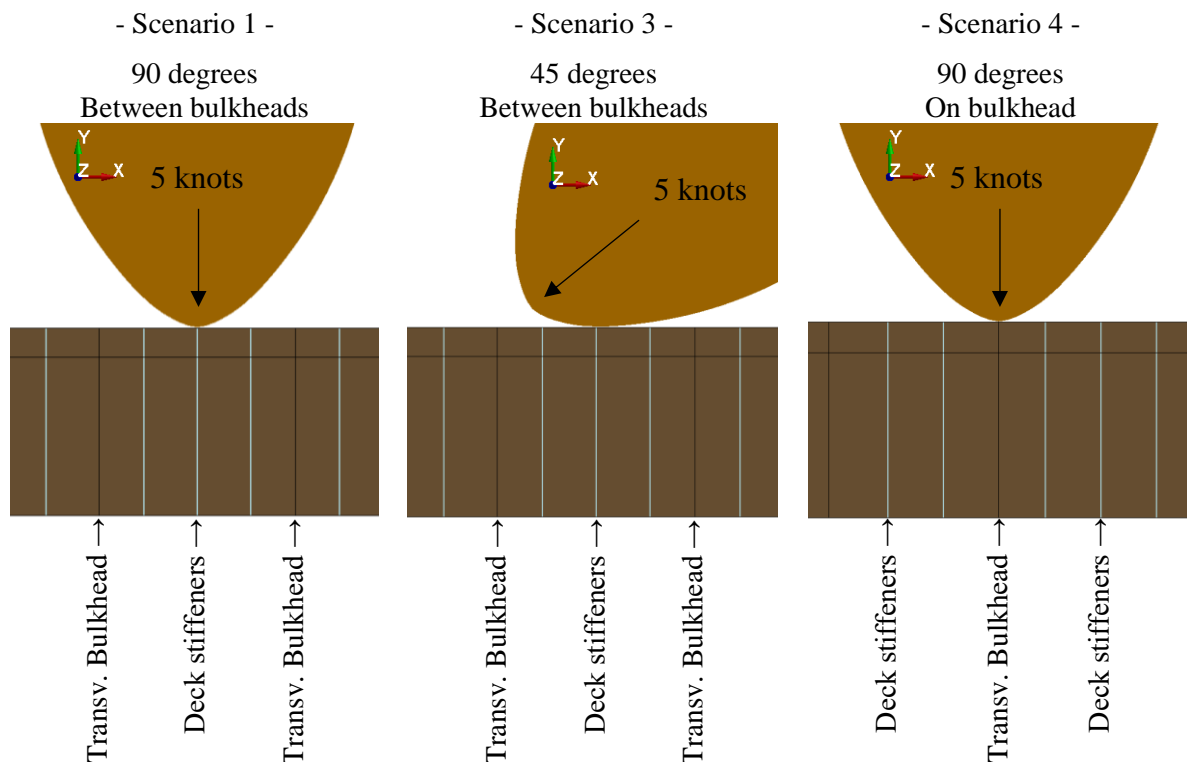

Figure 3.8. Collision scenarios for the validation

For each collision scenario, the parameters involved in the translation and rotation of the striking ship are automatically updated with the parametrization done in the previous section. Among these are, the position of the centre of gravity, velocity components and surge and sway vectorial directions. The collision scenario 2 of the Benchmark will not be considered for the validation, since collisions with large kinetic energy are not part of the analysis when initial velocity will be considered in the struck ship. Besides comparison of results is done without considering the results of the participant MARIN since there were no values for the time-evolution of the penetration and internal energy.

3.4. Results and comparison with Benchmark Study.

The validation of the collision simulation is done by comparing the time-penetration and internal energy evolution. Considering the elements that make up the striking ship are not deforming in the crushing process, the energy dissipated in the collision is determined by the internal energy of the deformed elements of the struck ship and the sliding energy produced by the frictional effect of the contact cards. The LS-Dyna code splits the effect of the sliding energy from deformation energy, and both are summed for the comparison. As mentioned in the benchmark study, this is not the case for SHARP calculation since the formulations to calculate the structural resistance due to plies or concertina tearing are based on experimentally validated closed forms.

3.4.1. Collision scenario 1

As shown in Figure 3.8, the first scenario is considering a perpendicular impact of a RoPAx running at 5 knots between two bulkheads around the midship section of a cruise ship at rest. Using the parametrized collision file detailed in Section 3.2.2, a real simulation impact of 8 [sec] is generated. A damage extent of 24.15 [m] length and 15 [m] height, including the bulb entrance, is generated by D3PLOTS, and it is shown in Figure 3.9. The stem and bulb shape of the striking ship is affecting the side of the struck ship at different heights. Besides, two effects in the crushing process are observed, first local damage in the side plate while struck is still at rest and later a second global effect coming from the imminent entrance of the striking ship. The latter effect is better observed in Figure 3.10, in which after 8 [sec] of simulation the struck ship is subjected to both sway and roll motions.
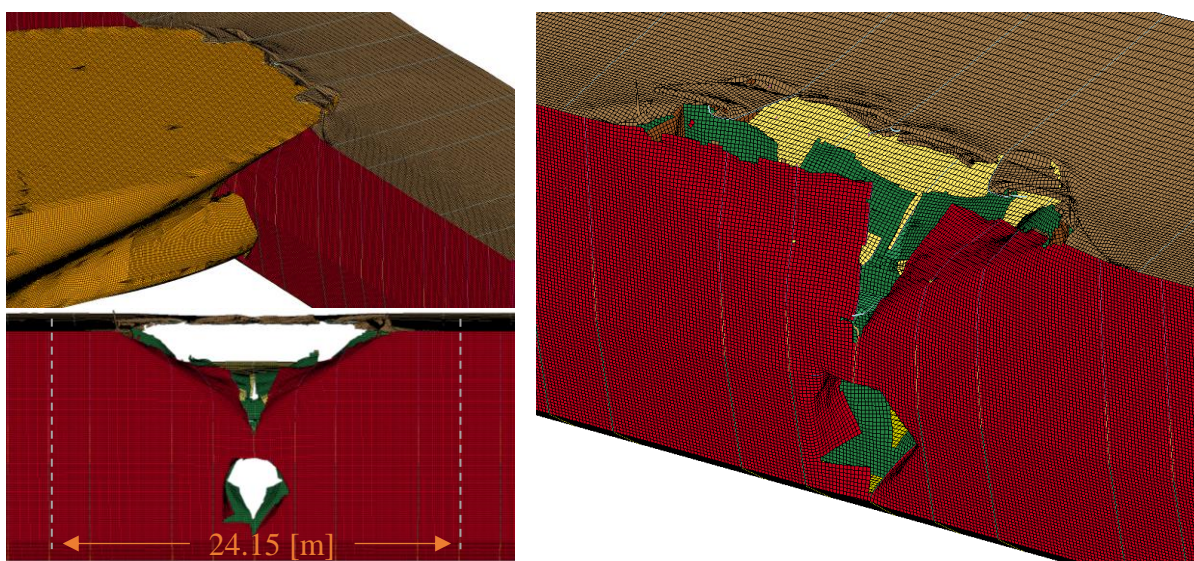

Figure 3.9. Extent of damage of Scenario 1

It was observed in the simulation that after 3 [sec] of penetration, the struck ship started being affected by the global dynamic movement on its sway direction. The surge velocity of the striking ship and sway velocity of the struck ship seems to be similar after 6 [sec] of simulation, then penetration is not increasing significantly. From the initial scenario, a total of 4 [m] displacement in the Y direction is estimated. Moreover, in the Front view (YZ) of Figure 3.10, is also noticeable an induced rolling movement in the struck ship as penetration increases.
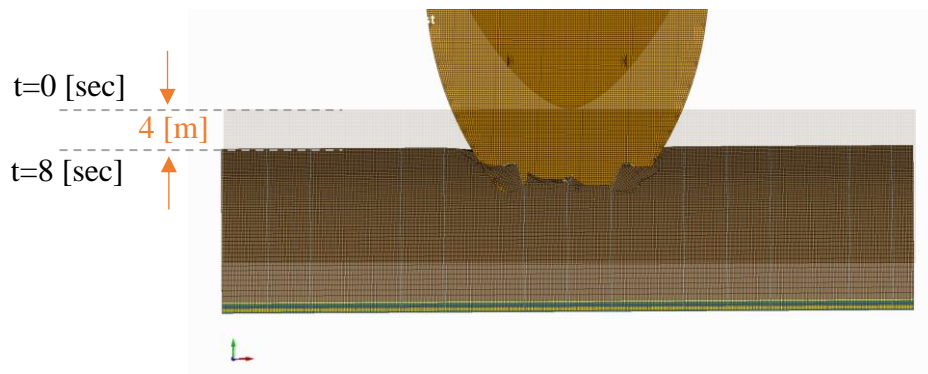
Top view (Plane XY) - Global displacement
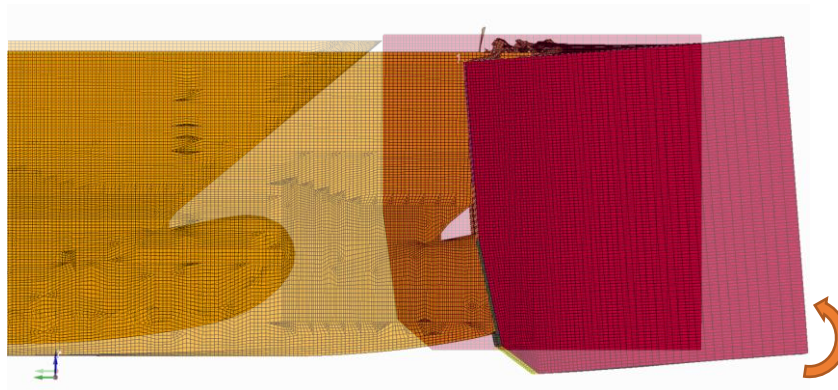
Front view (Plane YZ) - Global displacement

Figure 3.10. Global displacement of Scenario 1

Considering the Y displacement of two nodes and the internal energy of the deformed material plus sliding energy, the results of this scenario are compared. Total penetration of 9.85 [m] was obtained in the struck ship, measured from the side shell of the struck ship up to the last Y position of the bow tip of the striking ship deck.
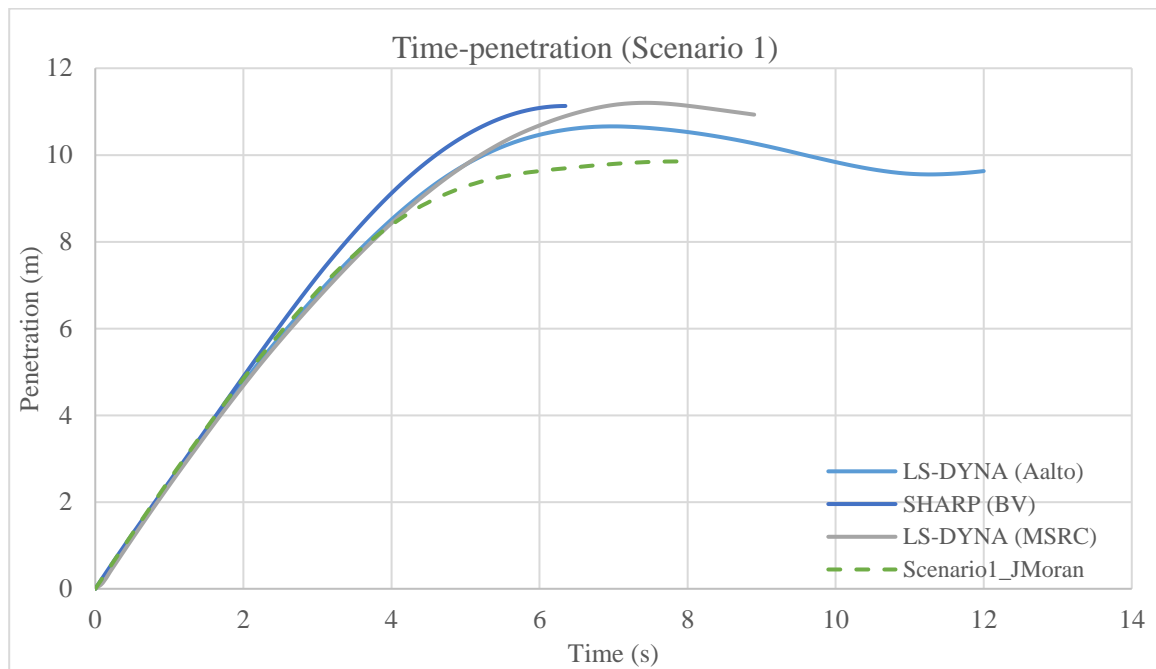
Figure 3.11. Comparison of time-penetration evolution - Scenario 1

The same rate of penetration is observed for the first four seconds of simulation and some differences are obtained in the maximum value. In Figure 3.11, a smaller value of maximum penetration is obtained for scenario 1 regarding all the results of the benchmark. The maximum difference of 12% is obtained when comparing with MSRC which was calculated using LS-Dyna. It is worth noticing that according to the reference study, the participants used a threshold strain value of 0.1 for all the collision scenarios while 0.2 was selected in the setup of this simulation due to the ration thickness-element size, as recommended in Section 2.4.1.
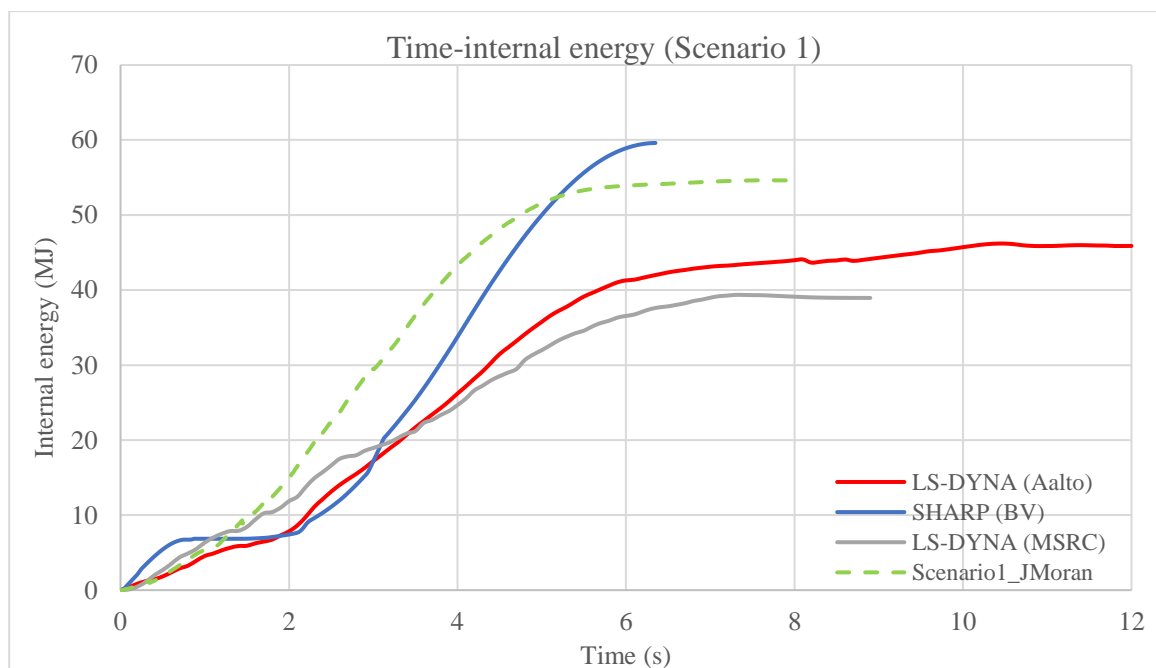

Figure 3.12. Comparison of time-internal energy evolution - Scenario 1

The major contribution of the internal energy evolution shown in Figure 3.12, is coming from the deformation of the elements than sliding. There is a clear difference in the results obtained in scenario 1 than those from the benchmark study from 2 to 5 [sec]. This difference may be influence by the rupture criteria assumed as double of the reference value as explained in the material card definition, see APPENDIX A1.

More deformation energy contribution is obtained from the elements before reaching the failure strain threshold. In the internal part distribution, the side shell, upper deck, and inner side are the elements that have contributed more to the total internal energy respectively. A maximum value of 54.6 [MJ] is reached with this simulation, compared with a higher of 59.6 [MJ] from SHARP and a lowest of 39.34 [MJ] from MSRC calculated with LS-Dyna.

3.4.2. Collision scenario 3

For scenario 3, the striking ship is impacting at 45 [deg.] concerning the surge direction of the struck ship with an initial velocity of 5 [knots] as presented in Figure 3.8. The extent of damage is more longitudinal compared with the perpendicular impact of other scenarios as shown in Figure 3.13. The total length of the damage is 29.6 [m] and only 4.8 [m] height compared to scenario 1 since no entrance of the bow bulb is appreciated, see Front View in Figure 3.14.
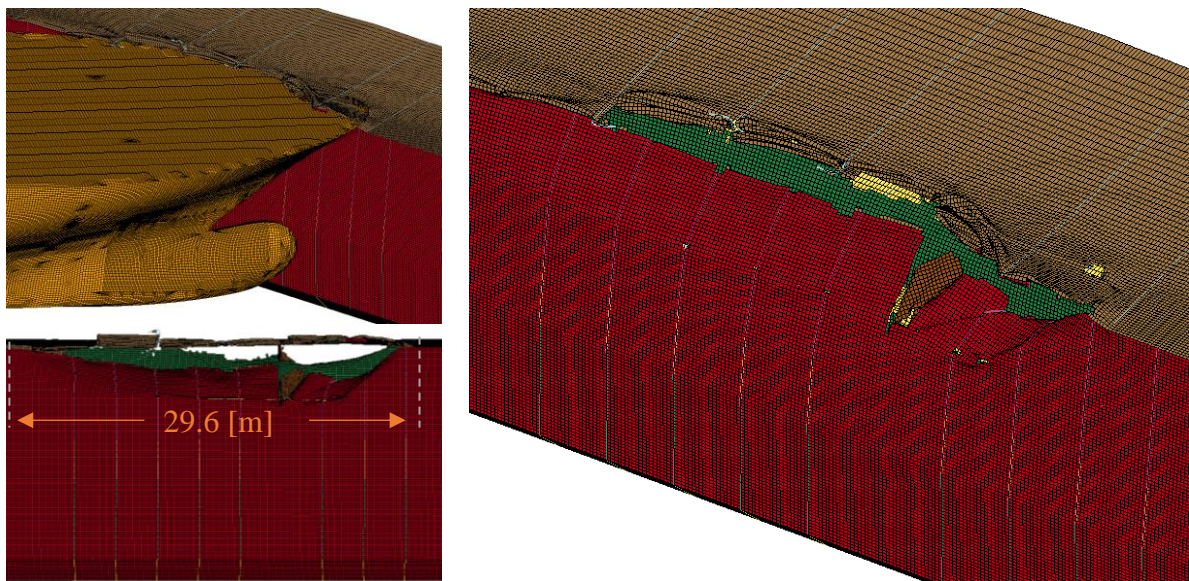
Figure 3.13. Extent of damage of Scenario 3

The perpendicular penetration length into the struck ship is expected to be lower than right-angle collisions. Due to the longitudinal damage, the transversal bulkhead located at 112.4 [m] as denoted in Figure 3.1, was affected in between the upper deck and the immediate lower one. In Figure 3.14, the action of the global displacement is appreciated from two perspectives. The struck ship has yaw, sway, and roll movements regarding its rest position. After 8.0 [sec] of

simulation, a small variation in the surge direction of the striking ship was observed, and a combined movement together with the struck ship in the last 3 [sec].
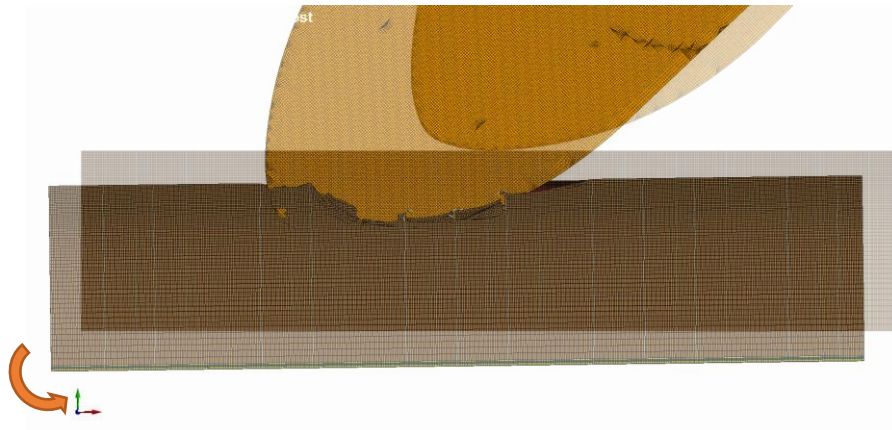
Top view (Plane XY) - Global displacement
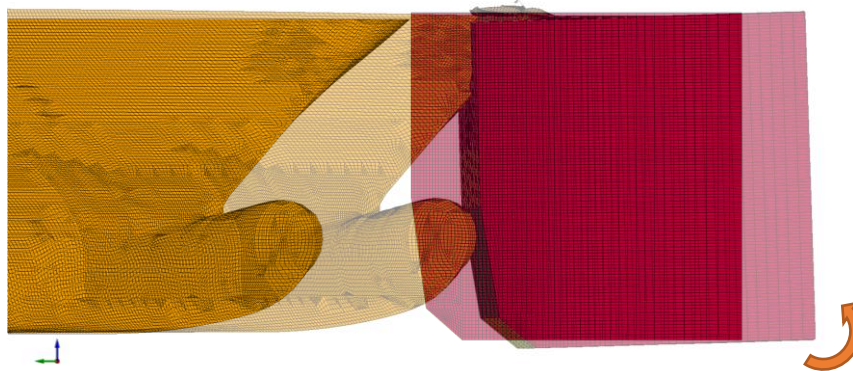
Front view (Plane YZ) - Global displacement

Figure 3.14. Global displacement of Scenario 3

The maximum penetration perpendicular to the side of the struck ship was 5.0 [m] at the end of the simulation. It is observed in Figure 3.15, the maximum difference in the penetration length of 6,9 [m] is with SHARP calculation at 4,8 [sec]. Regarding the minimum value, lower penetration of 3,8 [m] is obtained with LS-Dyna at 4 [sec] reported by MSRC. The smaller difference of 15.4% is regarding AALTO results but reached at 5.6 [sec]. The influence of the sliding energy restricts the penetration length in this case since it is more important than in right-angle collision cases.
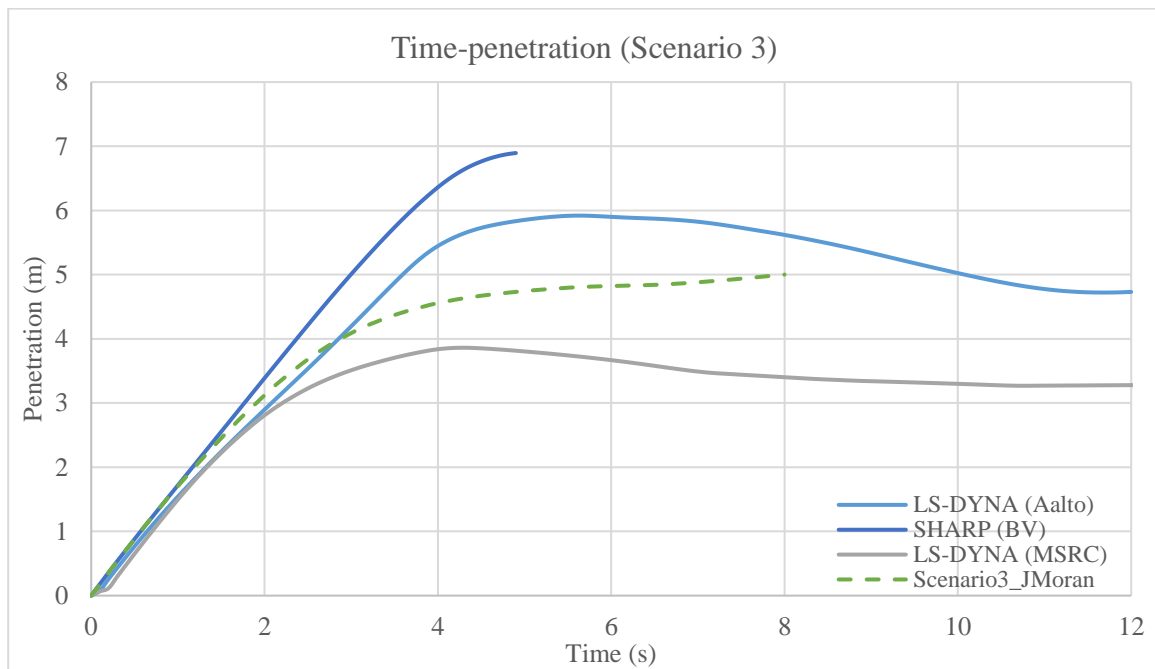
Figure 3.15. Comparison of time-penetration evolution - Scenario 3

There is a great contribution of the sliding energy in the total internal energy in this collision scenario. The sliding energy represents around 35% of the overall dissipated energy shown in Figure 3.16 for the current scenario. Besides, the structural components that are contributing most of the deformation energy are the side shell and the upper deck. Finally, the maximum internal energy of 52 [MJ] is obtained being up 50% more than the benchmark maximum results. This result may be related to the difference in the failure strain considered as double of the reference value to have a more realistic rupture of the material as justified in Section 2.4.1.
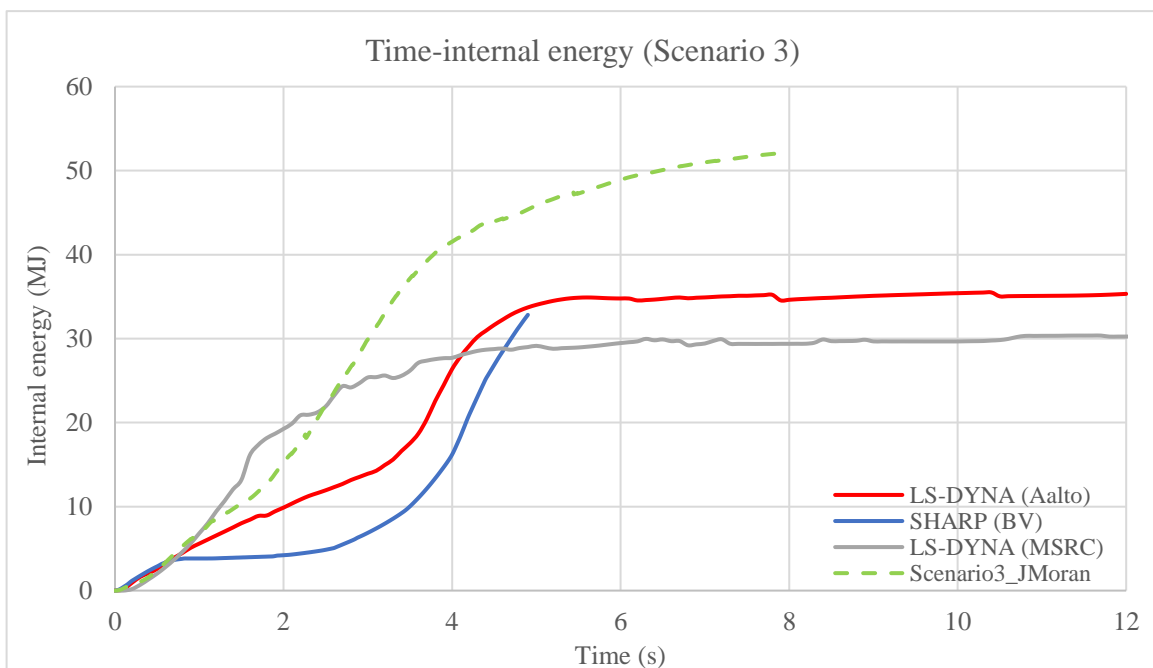
Figure 3.16. Comparison of time-internal energy evolution - Scenario 3

3.4.3. Collision scenario 4

A perpendicular collision at 5 [knots] on a transversal bulkhead of the struck ship is simulated in scenario 4. A smaller damage extent length of 22 [m] is found, compared with Scenario 1 while all the side height is affected since there is some bulb penetration see Figure 3.17.
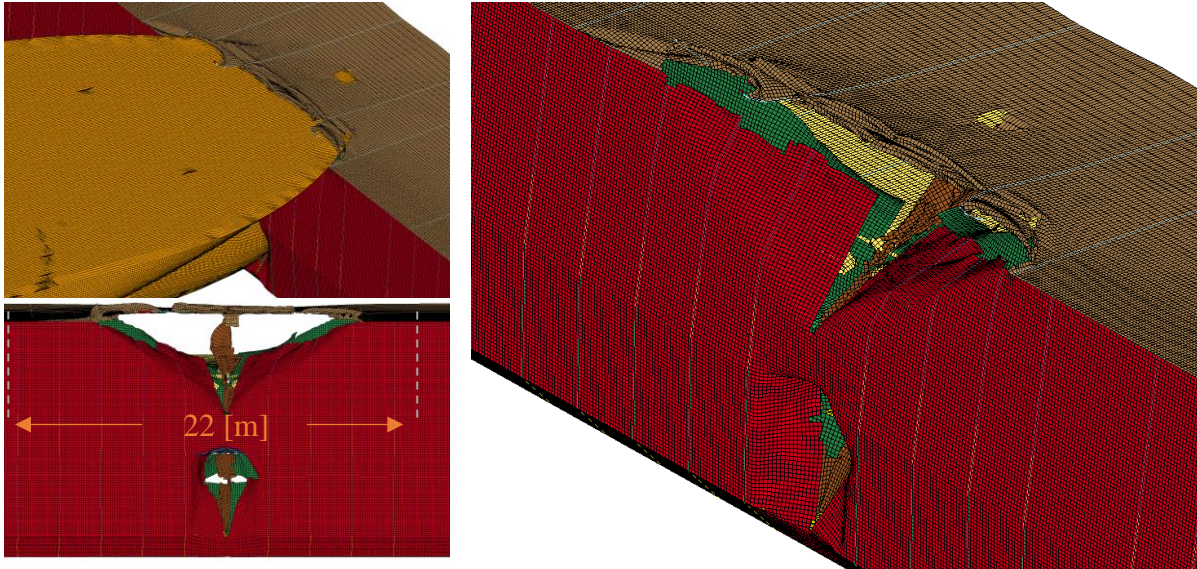
Figure 3.17. Extent of damage of Scenario 4

Most of the penetration induced by the local damage in the side shell is made up to 5 [sec] of simulation and then the global rigid displacement is activated in the following 3 [sec]. The effect of the latter can be seen in Figure 3.18, where mainly sway, yaw and roll movements are globally displacing the struck ship due to the impact, while for the striking ship, the surge motion has been reduced. A bigger influence in the global displacement is visible when comparing with scenario 1. An average sway movement of 4.5 [m] is found in the struck model. Since the impact is not around the centre of gravity of the ship, a yaw movement is evident with a bigger displacement to the aft part of the ship.
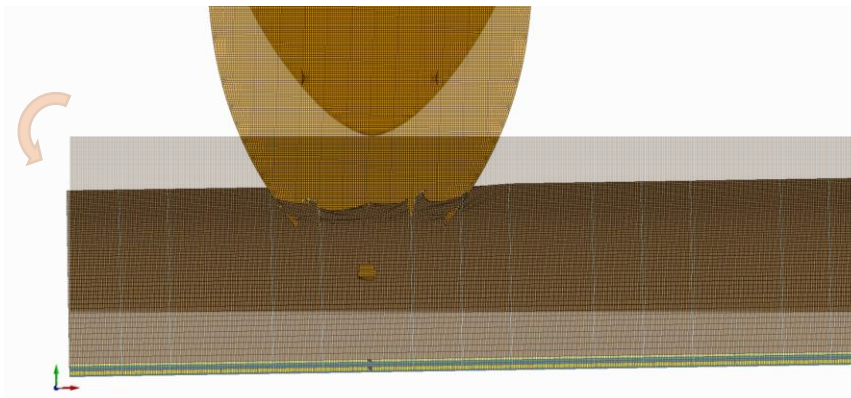
Top view (Plane XY) - Global displacement
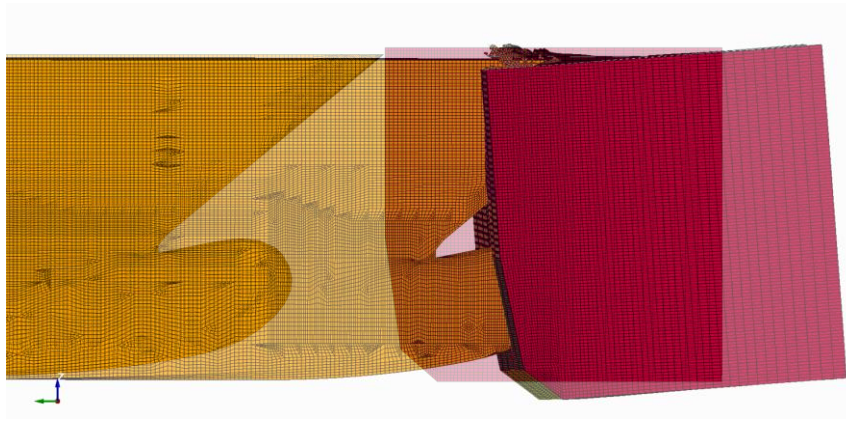
Front view (Plane YZ) - Global displacement

Figure 3.18. Global displacement of Scenario 4

For the first 3 [sec] of simulation similar penetration rate is obtained when considering SHARP calculation, however, the maximum values of penetration differ from 9.13 [m] of this simulation to 8.0 [m] obtained with SHARP. Regarding the calculations made by MSRC, the gap is smaller with a maximum of 8.55 [m] although reached at 5.5 [sec] of simulation.
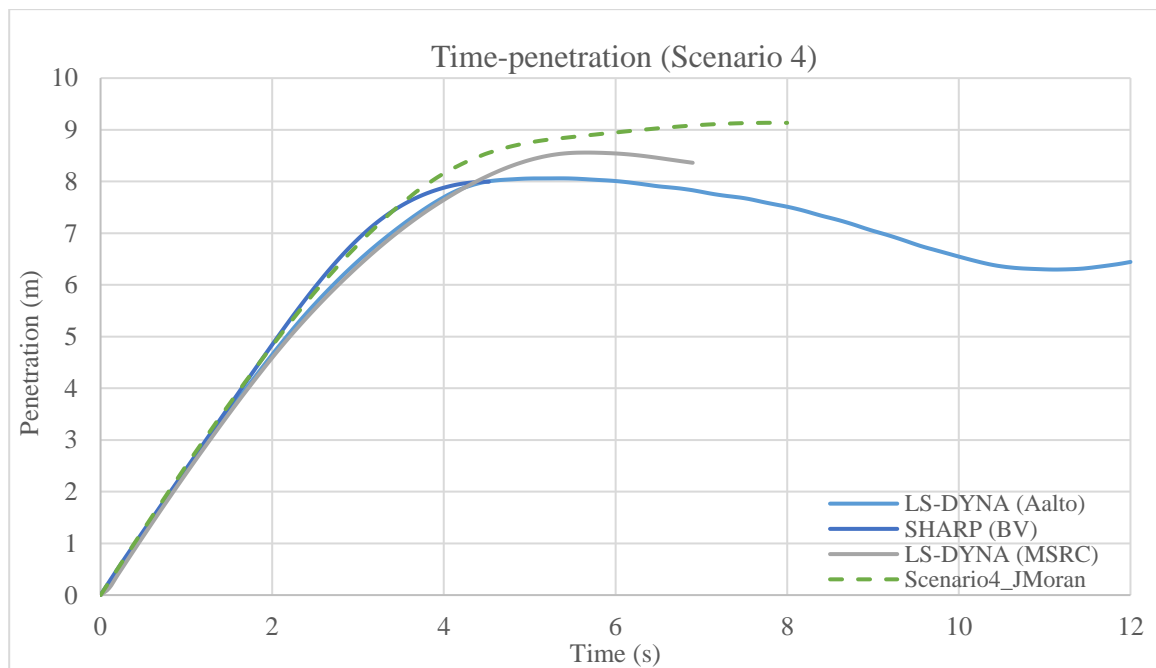
Figure 3.19. Comparison of time-penetration evolution - Scenario 4

The transversal bulkhead located at the impact position is the third element dissipating more deformation energy after the side shell and the upper deck respectively. For the penetration length, a similarity is found with a maximum internal energy of 54 [MJ] in the rate of internal energy dissipated before the 8 [sec] about SHARP calculations, which has a maximum of 52 [MJ]. Larger discrepancies are found for other results also obtained with LS-Dyna, as can be seen in Figure 3.20.
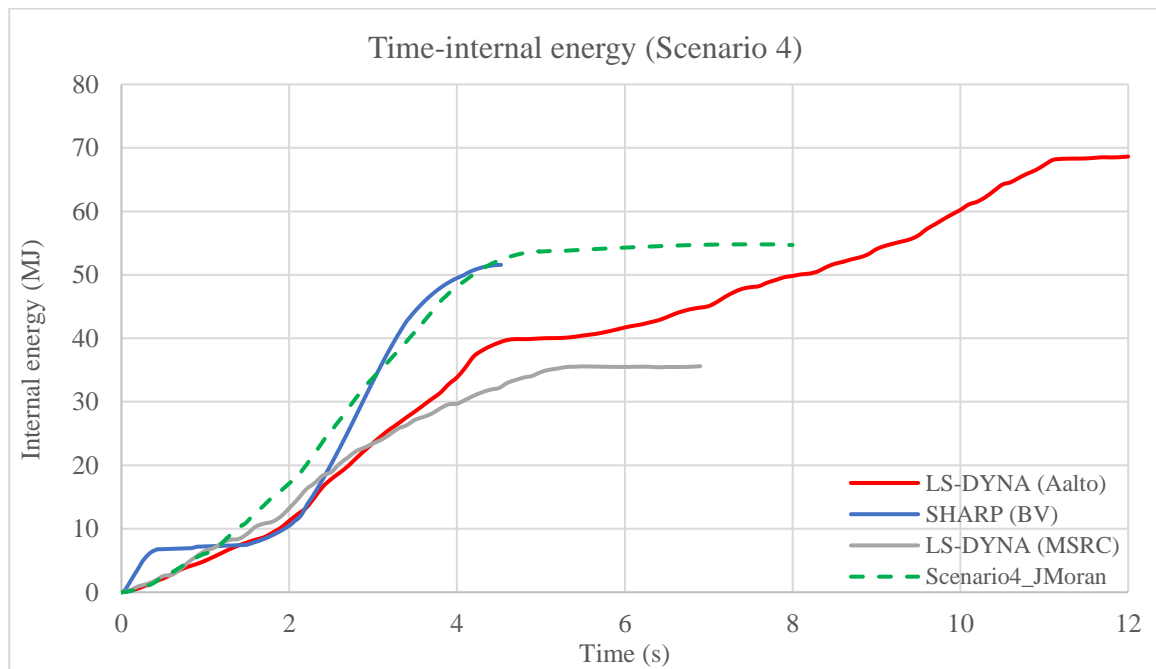
Figure 3.20. Comparison of time-internal energy evolution - Scenario 4

Finally, three scenarios were generated and compared with a benchmark study to rely on the simulation of more acute angle collision scenarios considering initial velocities for both striking and struck ships. The parametrization of the initial conditions of the collision scenario enhanced the generation of several collisions to fit with the reference study. There were more similarities for scenarios 1 and 4, which are right-angle collisions, but more discrepancies are found for the inclined one.

Even though it was observed different tendencies in the time evolution of the results, the evaluation in the prediction of a ship collision is based on the damage extent produced in the struck ship. In the following tables, the maximum values of the benchmark study, are compared for the maximum values obtained in the simulation JMorán, in shaded cells. Positive values mean an increase from the reference value and vice versa.

Table 3.3. Percentage comparison for Scenario 1

(difference %)	LS-Dyna			SHARP
	Aalto	MSRC	JMorán	BV ICAM
Max. Penetration	-8%	-13%	9.8 [m]	-12%
Max. Internal Energy	18%	39%	54.6 [MJ]	-8%

Table 3.4. Percentage comparison for Scenario 3

(difference %)	LS-Dyna			SHARP
	Aalto	MSRC	JMorán	BV ICAM
Max. Penetration	-15%	30%	5.0 [m]	-27%
Max. Internal Energy	48%	71%	52.0 [MJ]	58%

Table 3.5. Percentage comparison for Scenario 4

(difference %)	LS-Dyna			SHARP
	Aalto	MSRC	JMorán	BV ICAM
Max. Penetration	13%	7%	9.13 [m]	14%
Max. Internal Energy	-20%	54%	54.7 [MJ]	6%

When considering the maximum penetration in the struck ship as a physical problem, for instance in the case of environmental pollution, a modest prediction is obtained with the simulation since smaller differences are obtained when comparing to the internal energy dissipated in the collision. The prediction in the penetration may be said to be better even when right-angle collisions are assessed, as seen for scenarios 1 and 4 for the same striking velocity. For scenario 1 is observed that 13% smaller penetration is obtained compared with all the reference values. In the case of scenario 4, when the transversal bulkhead is impacted opposite tendency is obtained since higher penetration is obtained being up to 14% greater than the reference. Good agreement is found for both cases since the difference is small.

Larger differences are obtained when oblique collisions are predicted with both methods. In Figure 3.15, the time-penetration of scenario 3 shows how the discrepancy appears after 2 [sec] of simulation for all the participants. It seems that the sliding of surfaces makes difference in the calculation process and the influence of it can be observed also for the internal energy evolution of the same scenario. Sorely there is no information on the sliding energy contribution from each participant to detach the analysis more deeply and analyse the contribution of each element to the global internal energy. The difference in the use of a greater threshold value for the failure strain of the material implies higher internal deformation energy, nevertheless, a more realistic prediction of the physical damage is expected.

The maximum internal energy of the system is heavily influenced by the rupture criteria assumed for the material. The deformation energy is expected to increase since the deformation of the elements absorbs more energy before the strain calculated reaches the threshold value. The effect of it can be observed in all the time internal evolution graphs when comparing the LS-Dyna results with exception of AALTO results that presents a peak after 11 [sec] of simulation. Again, larger differences are found for the oblique collision, nevertheless, difference tendency is also presented between the finite element participants. Despite that, a similar maximum internal energy is obtained in their results. Considering there was a difference for the rupture criteria assumed higher to get more realistic prediction based on the recommendation of (Simonsen & Lauridsen, 2000), the simulation file generated is used for the generation of new collision scenarios to assess acute-angle collisions of ships and to find differences with the SHARP program.

3.5. Definition of acute angle collision scenarios.

The possibility of acute-angle collision scenarios considering initial velocity in the struck ship is analysed in this section. In the previous section, a 45 [deg.] collision scenario was generated to fit with the benchmark study, but some discrepancies were found both for penetration and internal energy. Two more collision scenarios are considering for the analysis of inclined collisions but now also considering an initial velocity of 5 [knots] in the struck ship. An acute-angle arrangement is set up for these as shown in Figure 3.21. The first scenario is to study the opposite direction between the two ships with an initial angle of 30 [deg.] concerning the horizontal for the striking ship running at 5 [knots]. A second scenario is looking at the same direction collision but at 150 [deg.] regarding the X-axis.
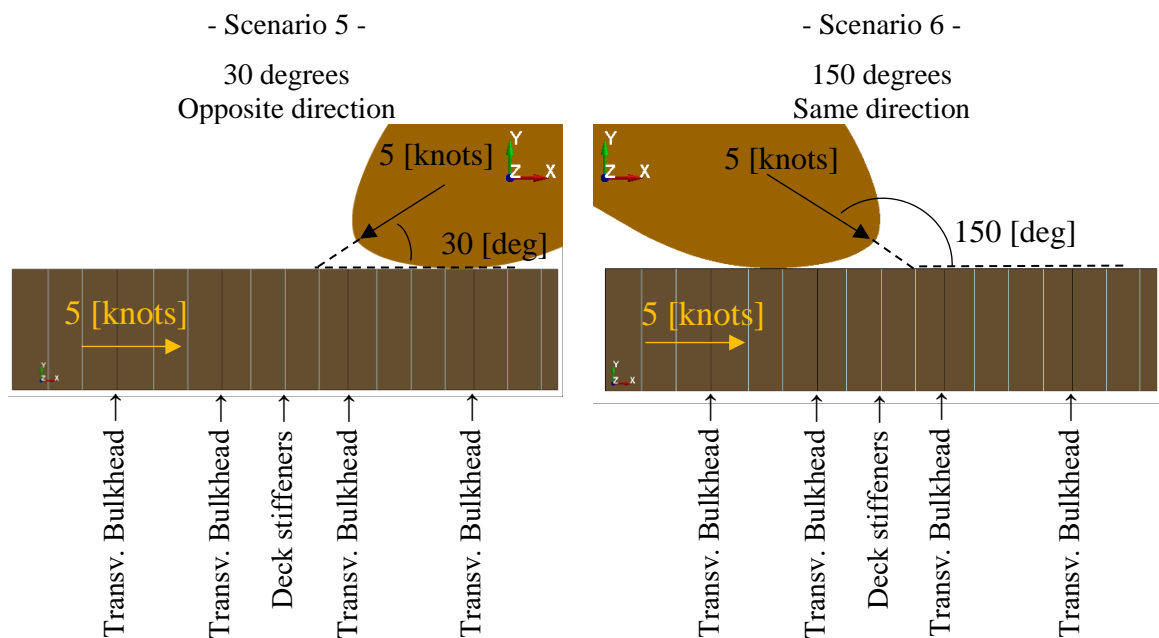
Figure 3.21. Description of the extreme collision scenarios

The striking ship is initially located close to the rigid bulkheads since a longer extent of damage is expected but preventing interaction with them to avoid overreaction in the struck ship response. There may be an induced unrealistic stiffness in the zone of interest due to the nondeformable parts. For the opposite direction collision, the rate of damage is likely to be wide along the side of the struck ship but smaller than for the same direction case where both ships are projected to advance stuck together. The results of these simulations will be compared with those obtained with the SHARP program after the presentation of the simulation sketches.

3.5.1. Collision scenario 5 (LS-Dyna)

When both ships collide following opposite directions, almost all the side shell of the struck ship is damaged at the main deck height of the rigid striking ship as can be seen in Figure 3.22. Besides, there was no affectation in the bottom part of the struck ship due to the bow bulb. Despite 8 [sec] of simulation and the length of the damage extent, both ships did not stop their advance and if longer time simulation would be considered, there may be some interaction with the rigid bulkhead, however, the total penetration perpendicular to the side shell was 3.2 [m] being the length of damage more important and reaching 80% of the struck model length as shown in the following longitudinal view.

longitudinal view
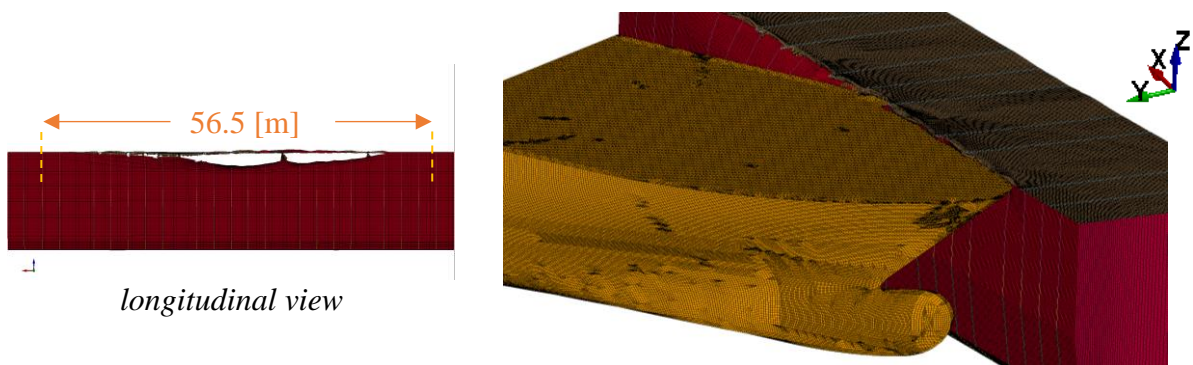
Figure 3.22. Extent of damage of Scenario 5 (LS-Dyna) Opposite direction
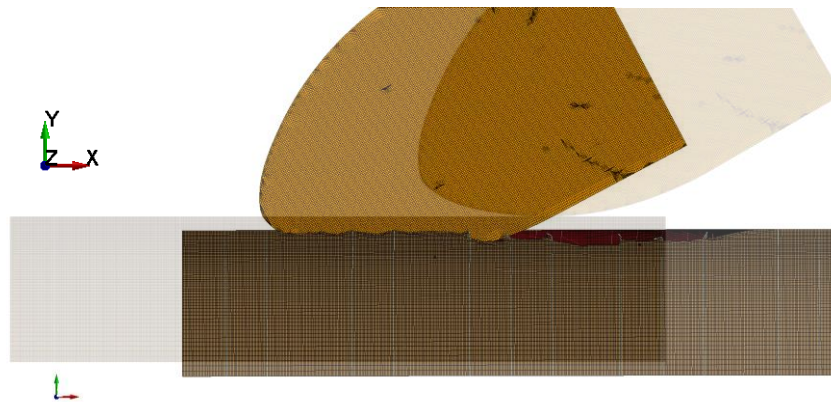
Figure 3.23. Global displacement of Scenario 5 - Top view (Plane XY)

There was a variation in the initial direction of the ships after the collision. Even though there is no coincidence between the final velocities of the struck and striking ships, a displacement in the sway struck ship direction and a smaller one in the surge direction of the striking ship is noticeable in Figure 3.23.

3.5.2. Collision scenario 6 (LS-Dyna)

In this simulation is generated a collision scenario with both ships going in the same direction both with an initial velocity of 5 [knots] as shown in Figure 3.21, with the first impact point at 89.8 [m] from FP of the struck ship, see Figure 3.1. There was half of the damage extent length

from the previous case since only local penetration of 1.93 [m] was obtained. The external dynamics of both ships is noticeable when there is a change in the initial direction, see Figure 3.25. After the global motion of the rigid bodies, the striking ship changes its surge direction detaching from the struck ship.
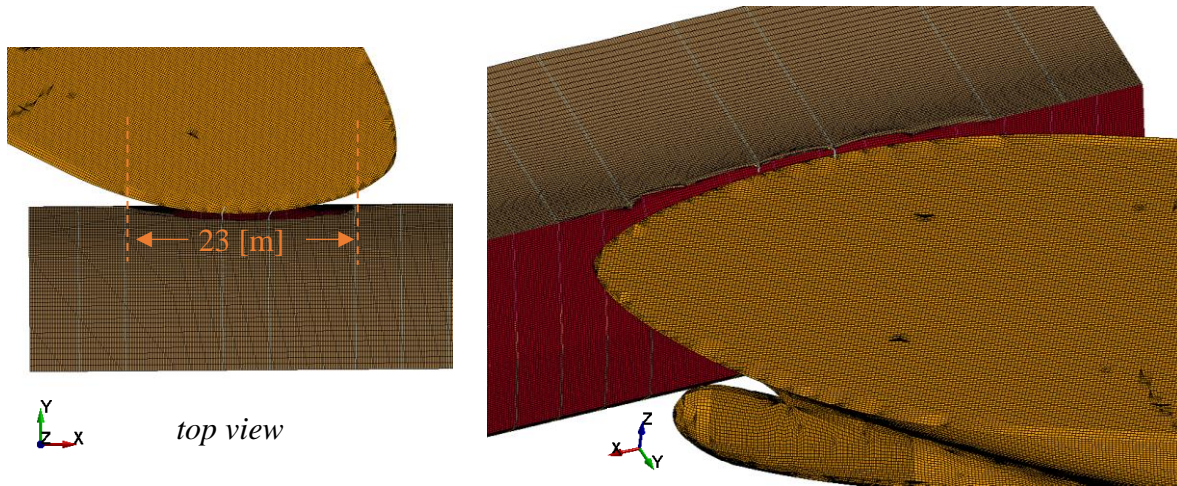
Figure 3.24. Extent of damage of Scenario 6 (LS-Dyna) Same direction
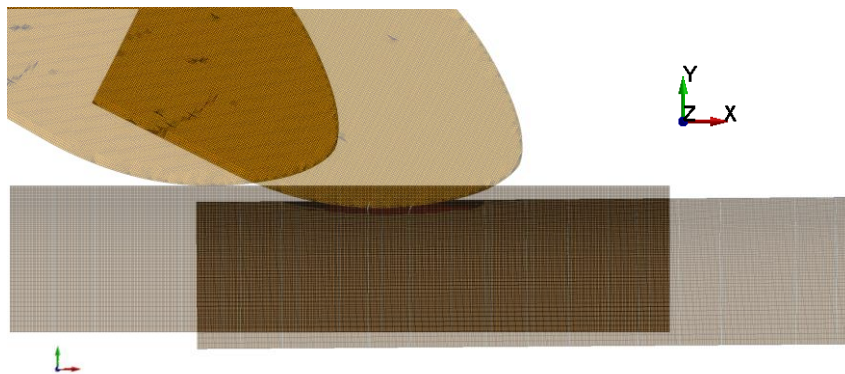
Figure 3.25. Global displacement of Scenario 6 - Top view (Plane XY)

Even though a smaller penetration was obtained in this collision scenario, a similar global displacement was obtained compared to the previous scenario. The impact of both ships with and against similar directions seems to have the same inertia interaction as rigid bodies as shown in Figure 3.25 and Figure 3.23. The struck ship is being affected by a sway displacement with some small yaw. While for the striking ship, a small reduction in surge velocity is noticed after the impact of 8 [sec]. The results of penetration and internal energy evolution are compared in section 3.7 to assess the usage of other rapid software for the same collision eventuality.

3.6. Simulations with the SHARP program.

To evaluate the performance of the SHARP program for the analysis of ship collisions, the penetration and internal energy evolution of previous scenarios are reproduced and compared. The simulation of the impact scenario consists of the modelling and structural interaction of two simplified hull forms defined by parametrized geometries. The striking ship is modelled by the definition of both idealized bow and bulb shapes. The parameters as bulb length, height and transversal radius define the bulb geometry, while for the bow shape, deck longitudinal and transversal radius. For the struck ship definition, more detailed elements are required. The hull plates are defined by four patches corresponding to the different side shell thicknesses. The stiffening system is also specified by spacing and profile sections. In Figure 3.26, the general arrangement of a perpendicular collision is presented with the parametrized elements. The collision zone is defined between the two extreme bulkheads considered as rigid elements for the LS-Dyna simulations.
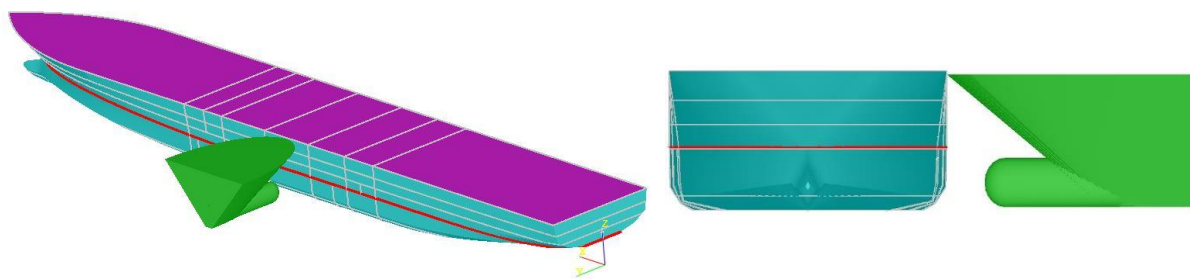
Figure 3.26. Perpendicular collision scenario with SHARP program

The two scenarios defined in Figure 3.21 are easily generated from the perpendicular one shown previously. The initial angle and the longitudinal position of the impact are the parameters set to 150 [deg.] and 126.9 [m] for collision scenario 5, see Figure 3.27, while 30 [deg.] and 89.9 [m] for scenario 6 respectively. The material characteristics are set the same as for the finite element approach, including the rupture strain as 0.2. These parameters are following the system of reference designed in SHARP to match with the orientations set in LS-Dyna scenarios.

3.6.1. Collision scenario 5 (SHARP)

The collision in the opposite direction of the ships is simulated after the automatic generation of the super elements and the quick solving procedure of 231 iterations. The process is expected to stop when the surge velocity of the striking ship at the impact point becomes lower than the sway velocity of the struck ship at the impact point. Crushing forces and the deformation energy are calculated at each step finally completed after 5.75 [sec] of simulation time with a total penetration of 3.82 [m] measured from the side of the struck ship.
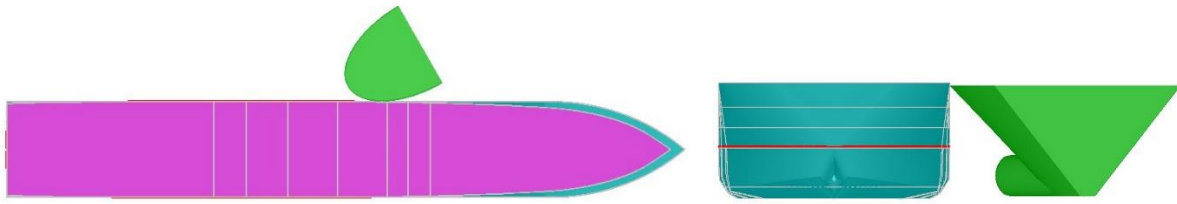
Figure 3.27. Set-up of collision scenario 5 (SHARP) Opposite direction

Three types of super elements were involved in the calculation of the crushing forces and deformation energy. The side shell, side stiffeners and transversal bulkheads are being affected due to the impact of scenario 5. However, only some side stiffeners completely failed in the indentation process as shown in Figure 3.28a, where failed elements are coloured in red. There was also a small deviation in the global displacement of both ships due to their interaction. A sway movement in the struck ship and some modification in the surge direction of the striking ship as mainly noticed in Figure 3.28b.
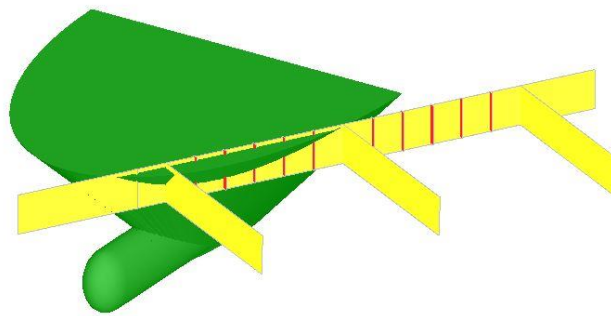
(a) Super elements involved in the extent of damage
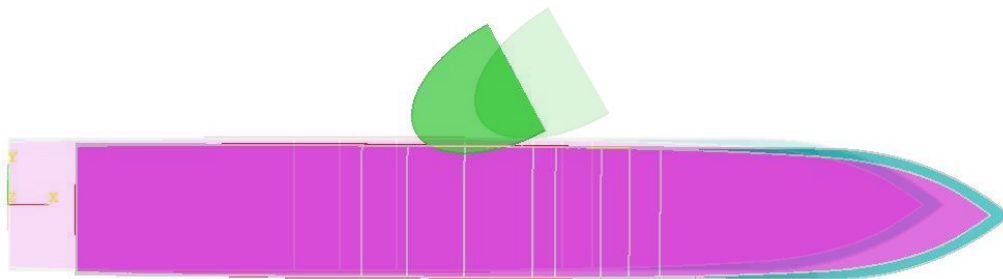
(b) Global displacement

Figure 3.28. Result of collision scenario 5 (SHARP) Opposite direction

The results of internal energy and penetration are compared later with the results obtained by LS-Dyna for the same scenario. From the results, is possible to extract the individual contribution of each component to the global internal energy so that differences in the methods can be analysed in detail.

3.6.2. Collision scenario 6 (SHARP)

The collision scenario of both ships following the same direction is generated by changing the angle and longitudinal position of impact and results are obtained after 97 iterations, being quicker compared to the previous case. The total simulation time of the complete crushing process was 2.4 [sec] with a total penetration of 1.71 [m] from the side shell of the struck ship.
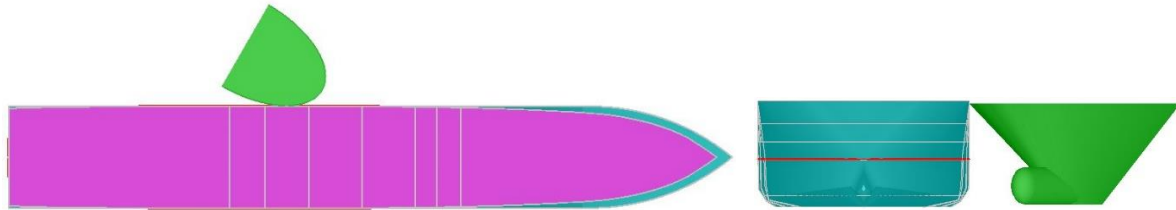
Figure 3.29. Set-up of collision scenario 6 (SHARP) Same direction

A total of three super elements are resisting the indentation process of the striking ship. The side shell, transversal bulkheads, and stiffeners are contributing to the deformation energy of the collision. As shown in Figure 3.30a, the side shell is the only super element that fails in the solution, since it is coloured red. A smaller global motion is described in Figure 3.30b in the struck ship when comparing to the previous collision scenario. The sway direction of the struck ship is less affected concerning its initial position, but more in the surge direction of the striking ship.
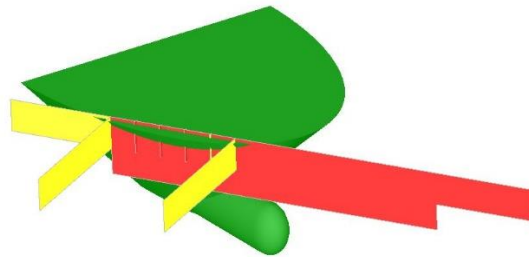
(a) Super elements involved in the extent of damage
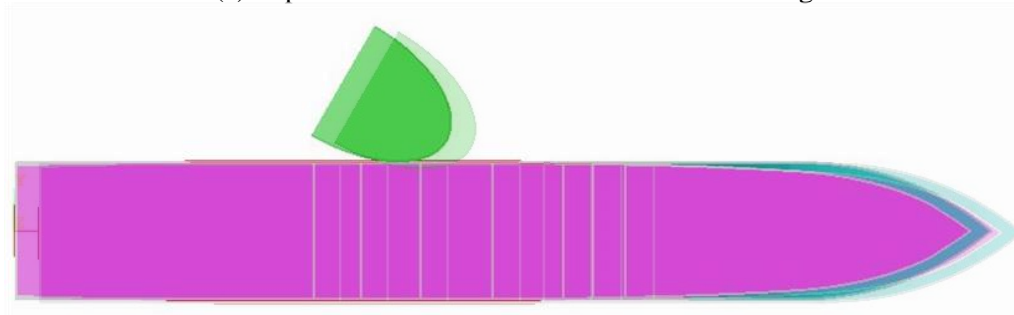
(b) Global displacement after the collision

Figure 3.30. Result of collision scenario 6 (SHARP) Same direction

A total damage length of 18.4 [m] in the direction of the struck ship side is obtained for this collision scenario. Besides, from the results, it is determined that one patch of the side shell is failing after 0.75 [sec] of simulation, thereafter, a second patch is contributing with an increment of the total internal energy developed in this collision scenario around 1.5 [sec].

3.7. Comparison and analysis of results

A complete penetration and internal energy evolution comparison from two collision scenarios considering both initial velocities of the struck ship is developed in this section. The time-penetration plot depicted in Figure 3.31, shows higher values for the indentation process into the struck ship when both ships collide following opposite directions since the damage extent is larger in both approaches. In the same graph, similar values for maximum penetration length are calculated at the same time. In the case of opposite collision, the program SHARP (solid lines) obtains higher values than those from LS-DYNA (dashed lines) while for the same direction collision there is an inverse tendency in the results of both approaches. The maximum values are reached before the end of the LS-Dyna simulations; a peak of 3.2 [m] at 5.8 [sec] for the opposite direction, while 1.9 [m] at 2.9 [sec] when both ships have the same advance direction. When using the super element method, higher penetration is got when both ships have opposite directions and are slightly smaller than finite elements for the same direction. However, it is worth noticing the good approximation of the SHARP program in estimating penetration length at a considerably less computational time.
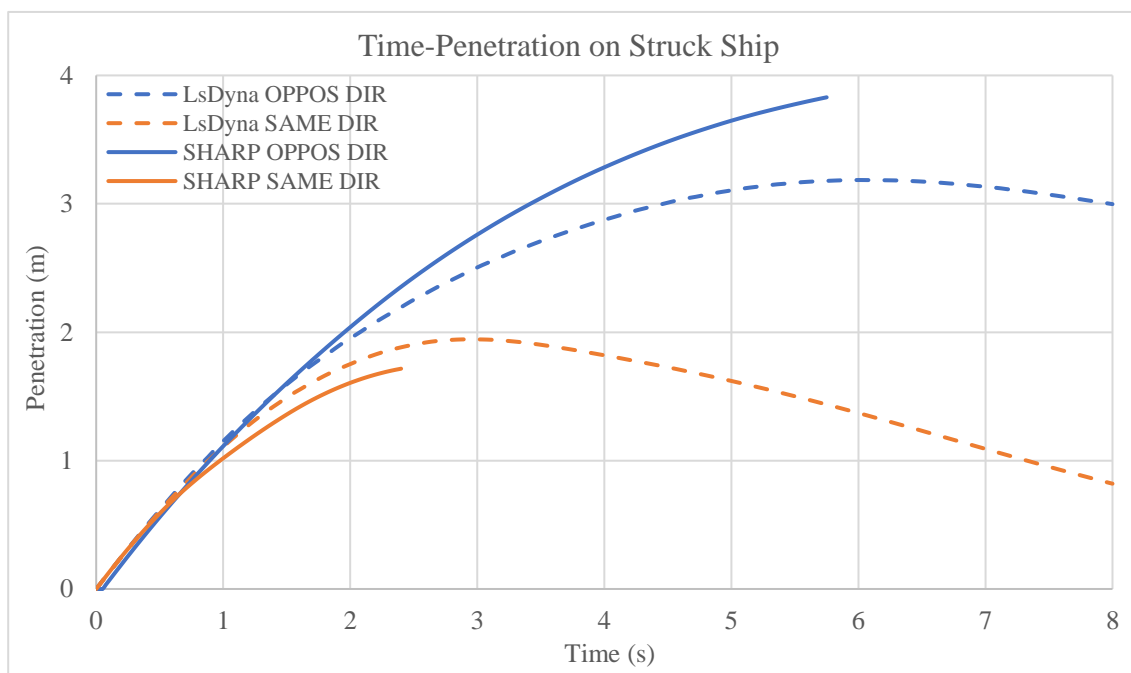
Figure 3.31. Comparison of time-penetration evolution

The super element-based software SHARP gets more conservative results than the finite element method when comparing the opposite collision scenarios of Figure 3.21. In this case, the time evolution obtained with SHARP details higher values than LS-Dyna. A discrepancy of 16% in the maximum penetration is got for the worst damage case as shown in Table 3.6 when both ships have opposite directions, at around the same simulation time of 5.8 [sec]. In the same comparison table, the large differences in the damage length are evident. On the other hand, a quite good approximation in the time-penetration, as well as the maximum value, is got when both ships have the same direction as shown in Table 3.7. A smaller difference in the damage length is found for this case.

Table 3.6. Maximum penetration and damage length comparison of Scenario 5

30 [deg.] Opposite dir.	LS-Dyna	SHARP	Difference
Max. Penetration	3.2	3.8	16%
Damage length	56.5	26.8	111%

Table 3.7. Maximum penetration and damage length comparison of Scenario 6

150 [deg.] Same dir.	LS-Dyna	SHARP	Difference
Max. Penetration	1.9	1.7	13%
Damage length	23.0	18.4	25%

The distinction of LS-Dyna between deformation energy and sliding energy is shown in Figure 3.32 to analyse the contribution to the great difference in the total internal energy regarding the SHARP program. There is a large difference in the internal energy dissipated for the finite element calculation when both ships impact in different directions. For this case, more than half of the internal energy comes from frictional energy dissipation. While for the same direction case, a smaller contribution from the friction is depicted in Figure 3.32b. This is due to the larger damage length also marked in Table 3.6 and Table 3.7 in which almost double of side shell is affected. A proper setup of the contact cards is crucial when more sliding contact between the elements is expected in the collision.

The SHARP program does not differentiate between deformation and sliding energy, but total internal energy is attained from closed-form analytical expressions. When comparing only deformation energy in Figure 3.32a similar tendency is visible but sliding energy is completely underestimated. For scenario 6, when both ships have the same direction, different results tendencies are observed. The internal energy calculated with SHARP is overestimating the values from finite elements reaching its maximum around 2.5 [sec] of simulation and compared with LS-Dyna it is completely coming from the deformation energy of its components. It is

worth noticing that less damage length is calculated for opposite direction collision than finite element and the difference of sliding energy is noticeable.

Figure 3.32 shows a comparison of the internal energy obtained for both collision scenarios. The maximum total energy of the opposite collision scenario is greater than the same direction scenario for both approaches. Even though there is a clear discrepancy between the finite element and super element method when analysing scenarios separately, more energy is dissipated for the opposite direction collision in both methods. The difference with the SHARP program is quite smaller than LS-Dyna when comparing scenario 6 to scenario 5, but almost the same maximum internal energy is dissipated according to the SHARP program for both cases.
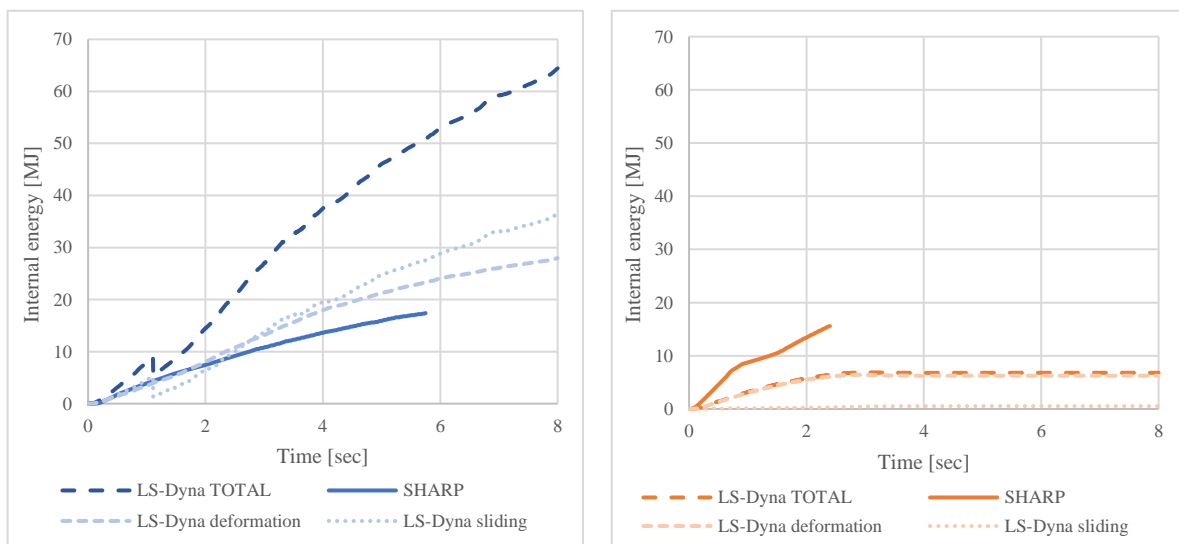
(a) Scenario 5 – Opposite direction   (b) Scenario 6 – Same direction

Figure 3.32. Comparison of time-internal energy evolution

An individual contribution of the deformation energy of the different parts of the struck could be obtained from the different software solutions. In Figure 3.33 is distinct the deformation energy that is contributed from the different parts to get the total deformation energy shown in Figure 3.32a. In the latter is worth to mention although total energy from LS-Dyna is greater than SHARP, is noticeable how more than three elements are contributing to the total deformation energy. In Figure 3.33b, in the SHARP program, no deck is collaborating in the deformation energy as shown for the LS-Dyna case. The total contribution is made with the super elements that have the chance to develop deformation based on the analytical formulations. While some resistance is coming from the elements that are globally interacting in the crushing process with the finite element method.

(a) LS-Dyna (b) SHARP
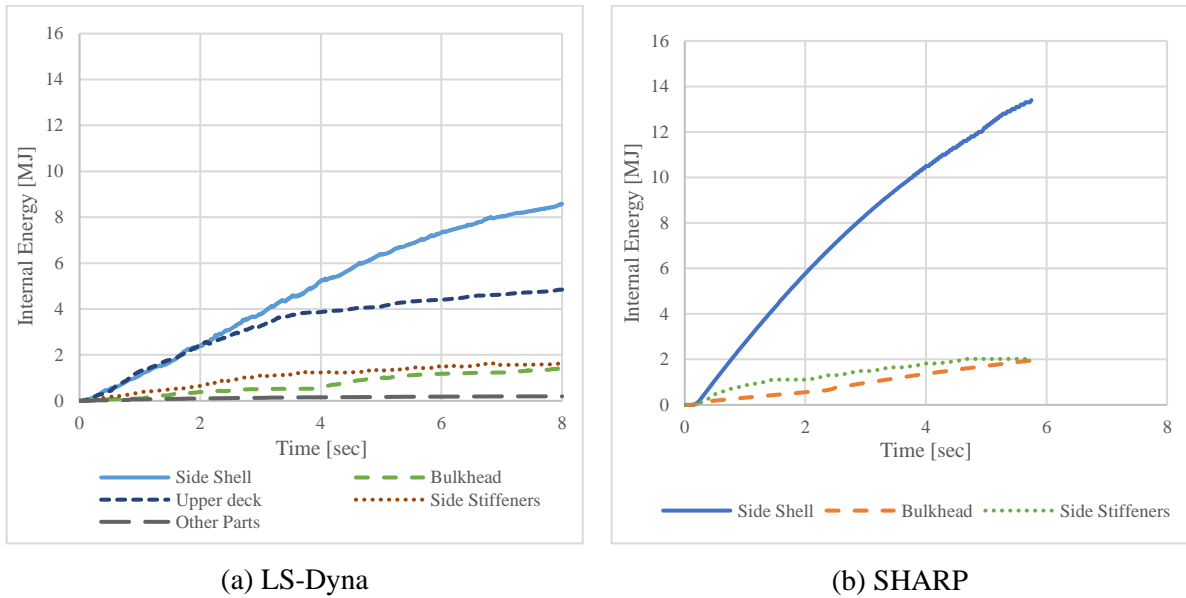
Figure 3.33. Part deformation energy contribution Scenario 5 (Opposite Direction)

Small sliding energy is contributing to the total internal energy for the same direction collision scenario, then a better comparison for the deformation energy by parts is made in Figure 3.34. On the side (b) of this graph, the SHARP program shows the failure for one patch of the side shell at 0.75 [sec] while there is a second contribution after, less than one second but without failing. An important contribution from the stiffening system is coming for this scenario, while LS-Dyna presents smaller participation for the side stiffening. It is worth mentioning there is a linear contribution of the different parts for SHARP, a direct relation between indentation and deformation energy is demonstrated for this super element method. Different constant behaviour is shown for the finite element approach since the striking ship is not increasing the indentation after 3 [sec] of collision.

(a) LS-Dyna (b) SHARP
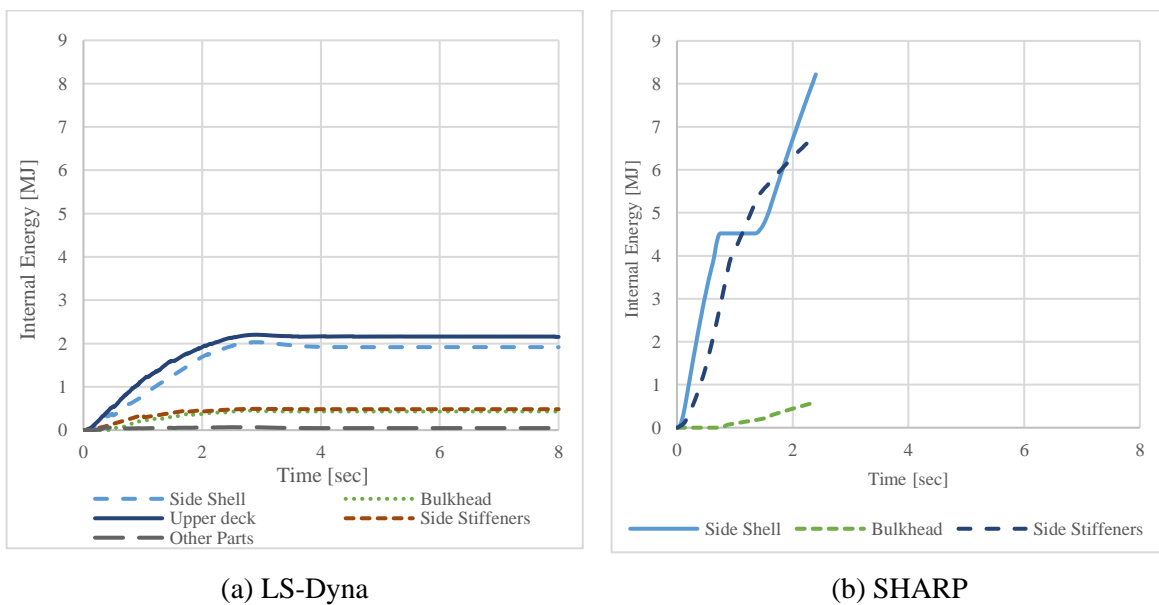
Figure 3.34. Part deformation energy contribution Scenario 6 (Same Direction)

Important differences in the internal energy estimation are found when comparing acute-angled collisions. The direct relation between indentation and absorbed energy is making differences in the super element method when sliding collisions are carried out. The super-element discretization made for the sliding collisions seems to make the struck ship model less stiff than calculations made by finite elements. This is making the striking ship go further in the penetration before it feels the global resistance of the struck ship.

The better prediction of the super-element method in a perpendicular collision than obliques is evidence in Figure 3.32, compared to the results of LS-Dyna. The contribution of the sliding energy may be expected as the same magnitude as the deformation energy when large contact of surfaces is involved according to the finite element method. When both ships have the same direction, the phenomena are expected to behave as a perpendicular collision guided by the perpendicular velocity component of the striking ship which would be small when narrow angles are formed between the ships.

The deformation energy calculated with the finite element method has a more independent contribution from the different parts of the struck ship. Is evident how the decks of the struck ship are having a heavy influence on the deformation energy. The close-form expressions implemented in the SHARP program are limiting the evaluation of more deformation energy coming from different parts that are affected in the collision. For instance, the deck plates of the struck ship are not having any participation in the deformation of the side shells since clamped edges are assumed for such types of basic super-elements, as presented in Section 2.5.2.

4. ANALYTICAL AND NUMERICAL MODEL APPROACH FOR THE SHIP PREDESIGN STAGE

The analysis of fortuitous collision scenarios is nowadays deemed in the ship design process since the early phase. As already mentioned, some accurate but also time-consuming procedures for the study of ship collisions are implemented with numerical simulations based on the finite element method. Some other analytical based simulations as the super-element method have been proposed and are worth being considered as faster but still under improvements to spreads its applicability. Nevertheless, the ship construction industry continues increasing and the safety of ships is a priority since the early design stage. It has become urgent for Shipyards to cover up this necessity by subcontracting special purpose companies which can study the crashworthiness of the ship. Currently, even one of the biggest worldwide shipyards is starting to employ efforts to perform collision analysis by themselves.

In the aim to define an analytical pre-design tool for the shipyard Chantiers de L'Atlantique, a collision case of a ship impacted on a gas storage hold is analysed. The event of a large-scale explosion is expected when a striking ship at high-velocity impacts and overpass certain limits in the structure of the struck ship which is at rest. The effect of internal mechanics is estimated through the collision resistance of the different crushed elements. The rapid formulation proposed by (Minorsky, 1958) and modified by (Perdesen & Zhang, 1998) based on experiments and statistics of accidents directly relates the energy absorbed with the volume of crushed material in the collision. Two types of energy absorption modes are used in this approach: plastic deformation due to plate tension and plate folding (Zhang, 1999).

The approach is based on the dissipation of the initial kinetic energy of the striking ship as plastic deformation of the damaged volume. Assuming the same rate of deformation energy is absorbed on both deformable ships, the kinetic energy is limited by the initial striking velocity to do not reach the threshold position of the gas tanks. Rapid estimation of the structural absorbing collision capacity with Minorsky formulations leads to an initial design criterion for the crashworthiness of a ship. One first procedure is proposed in this section for the estimation of a collision design parameter and then the generation of some collision scenarios using LS-Dyna code to analyse the influence of high-velocity impacts with future improvements for the analysis.

4.1. Analytical estimation of the penetration length.

A shared-energy design is proposed for the predesign of a ship collision event following (NORSOK Standard N004, 2004) for the design of steel structures against accidental actions. This design implies that both structures are contributing significantly to energy dissipation. For the case of ship-fixed structure collision, the effect is governed by the kinetic energy of the striking ship, and this is produced by the mass of the ship along with hydrodynamic added mass times the velocity of the ship as defined by Eq. 15. After the impact, some part of the initial kinetic energy may remain as kinetic energy while the remaining is dissipated as strain energy. Large plastic strains and serious structural damage is expected for both structures. The consequences in those effects may be determined either by non-linear dynamic finite element codes such as LS-Dyna or by the combination of energy considerations with simple elastic-plastic methods.

$$E_k = \frac{1}{2}(m_s + m_a)V_0^{\,2}$$ Eq. 15

When simple models are used for the estimation of the structural integrity of an installation, the considered dissipated energy as strain energy is represented in terms of the conservation of energy and momentum as shown in Figure 4.1. In this figure, the structural response is formally represented by the load-deformation relation in the event of a ship-fixed structure installation collision.
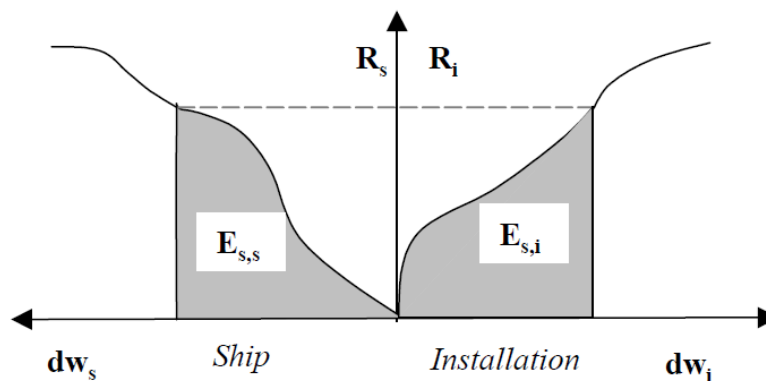
Figure 4.1. Dissipation of strain energy in ship and platform
Source: (NORSOK Standard N004, 2004)

The deformation energy curves in the function of the penetration length can be generated with the empirical energy methods studied by (Minorsky, 1958). These were later modified by (Perdesen & Zhang, 1998) and proposed three formulations to estimate the absorbed energy

after observation of the different basic failure patterns on experiments with sheet steel. For this estimation the plate cutting effect is not considered, reducing the deformation modes to plate tension (Figure 4.2a), and plate folding (Figure 4.2b). Considering the actual plate elements of the ships and the impact direction, the volume of material involved in the collision at each penetration step is approximated. Discretizing the main structural elements into two types of deformation patterns, the total energy at each penetration is determined. Stiffeners were not considered for this estimation.

(a) lateral loaded elements	(b) compression loaded elements

Figure 4.2. Deformation modes of plates elements

Source: (Zhang, 1999)

All the plate elements deforming within a lateral impact will suffer a plate tension effect and absorb an energy E_1 equal to:

$$E_1 = 0.77\varepsilon_c\sigma_0 R_T \qquad \text{Eq. 16}$$

From where ε_c is the critical rupture strain assumed as 20% for the failure criteria, σ_0 the flow stress of the material and R_T the volume of damaged material is assumed to deform as Figure 4.2a. Side shell, longitudinal bulkheads and longitudinal floors are specially considered when striking ship impacts perpendicular to the side shell of the struck ship.

As a second failure mode, the plate folding effect is considered for all the elements deforming as shown in Figure 4.2b. The energy E_2 is proportional to the volume R_T if the folded material but pointing out the relation thickness-width of Eq. 17 for each element. The flow stress of the material is again expressed as σ_0 and is obtained as the mean value of the yield stress and the ultimate stress of the material as recommended by (Pire, 2018).

$$E_2 = 3.5\left(\frac{t}{b}\right)^{0.67}\sigma_0 R_T \qquad \text{Eq. 17}$$

The energy contribution of the crushed elements by tension and folding deformation is now described as a function of the volume at each penetration step. Finally, the energies E_1 and E_2 from struck and striking ships are expected to absorb all the initial kinetic energy of the striking ship defined.

An idealization of the deformation pattern is necessary to assume a volume of damaged material while the striking ship is penetrating. In the plan view of Figure 4.3, a given number of penetration steps P_n are selected in the striking ship starting from the first impact point up to the end of the model. The corresponding width of each penetration w_n, is determined by the shape of the water plane of the striking ship at the same height of the struck ship's upper damaged deck. The same number of penetration steps and widths are later assumed to damage the struck ship positive from the first impact point to the centre line.
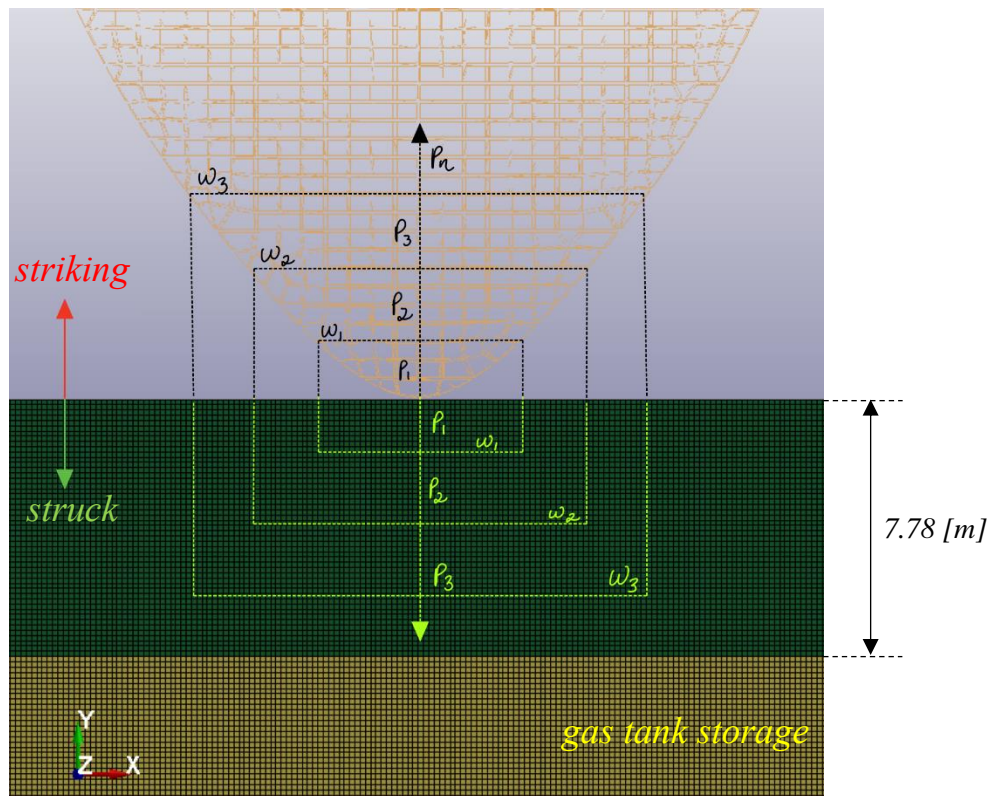
Figure 4.3. Deformation pattern assumed for both ships

The estimation of the damaged volume of the struck ship was implemented on a programming code following the algorithm shown in Figure 4.4 since mostly flat plates are managed. An external file is loaded to establish the limits and particularities for the vertical and horizontal elements to deform as folding plates since the energy calculation is related to the thickness and width of the element (Eq. 17). The crucial limit is represented by the green-yellow labelled representation in Figure 4.3 at 7.78 [m] from the side of the ship, at which the gas is stored.

The dotted box (legend):

σ_0; flow stress
ε_c; critical strain
P_n; penetration step
w_n; width step
P_e; max. element limit penetration
N_e; number of same elements
V_e; volume of element
R_x; total damage volume
E_x; total deformation energy

Energy estimation
Minorsky (1958),
Pedersen & Zhang (1998)

Data input

$\sigma_0, \varepsilon_c, th_{elements},$
$w_n = f(P_n)$
& element limits

Plate tension

Plate folding

horizontal elements   *vertical elements*

for all elements

$P_n > P_e, lim$

$P_n < P_e, lim$

$P_n < N_e, P_e \, lim$

yes   *no*   *yes*   *no*   *yes*   *no*

$V_e = f(th_e, w_n)$

$V_e = f(th_e, w_n, P_n)$

$V_e = f(th_e, w_n, P_n)$

$V_e = 0$

$V_e = f(th_e, w_n, P_{ne,lim})$

$V_e = f(th_e, P_{ne,lim}, N_e)$

$R_{t,h} = V_{n,e}$

$R_{t,v} = V_{n,e}$

$R_t = \sum_1^n V_{n,e}$

$E_{2h} = f(\sigma_0, th_e, w_n, R_t)$

$E_{2v} = f(\sigma_0, th_e, w_n, R_t)$

$E_1 = f(\sigma_0, \varepsilon_c, R_t)$

$E_{2H} = \sum_1^n E_{2h,e}$

$E_{2V} = \sum_1^n E_{2v,e}$

$E_{def}(P_n) = E_1 + E_{2H} + E_{2V}$

Figure 4.4. Flowchart for the estimation of the deformation energy of the struck ship

For the striking ship, the deformation energy is obtained with a manually volumetric measurement to consider the complexity in the curvature of the plates. At each penetration step, the volume is measured splitting between plates deforming in tension and folding. The hull plates are considered to deform as vertical folded elements and are included with elements such as decks and longitudinal bulkheads. For laterally loaded elements, all the perpendicular plates regarding the bow of the ship are considered. The deformation energy is calculated following the parameters involved for each type of folding element as regarded in Eq. 17. Finally, all the energy contribution from each deformed element at each penetration step along the complete model is added to the global striking ship deformation energy.

Table 4.1. Total deformation energy of the striking ship

Penetration [m]	Def. Energy [MJ]
0.6	8.3
1.1	16.8
2.3	34.6
2.8	42.3
3.9	60.9
5.1	80.4
6.2	101.0
7.3	117.6
8.4	138.1
9.5	156.2
10.6	175.1
11.7	270.8
13.4	311.1
15.1	351.7
16.8	432.5
19.0	513.9
21.6	831.7

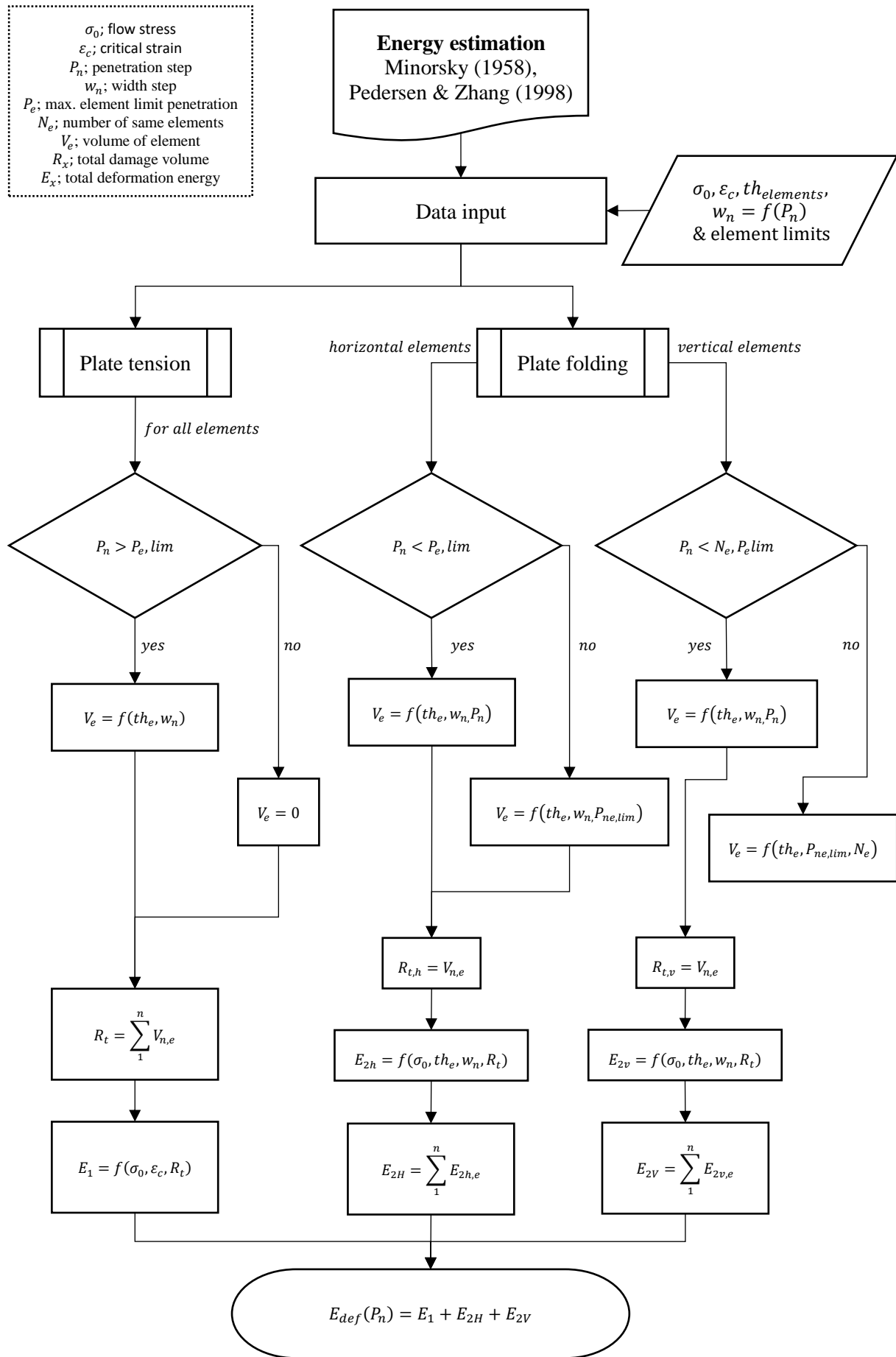Following a simple model description in which a significantly same rate of deformation energy from both ships is assumed, the shared-energy design proposed by (NORSOK Standard N004, 2004) is plotted in Figure 4.5. Assuming a negative direction of penetration in the striking ship, a simultaneous structural response of the collision event can be represented. The direct relation between the volume and the deformation energy is evident since for the same rate of deformation smaller energy values are got for the striking ship, in consequence, a flatter curve is plotted in the negative axis. However, a reasonable explanation is found due to different ship zones are considered for the impact, slimmer bow from the striking ship compared to box-like shape with a parallel midship section.
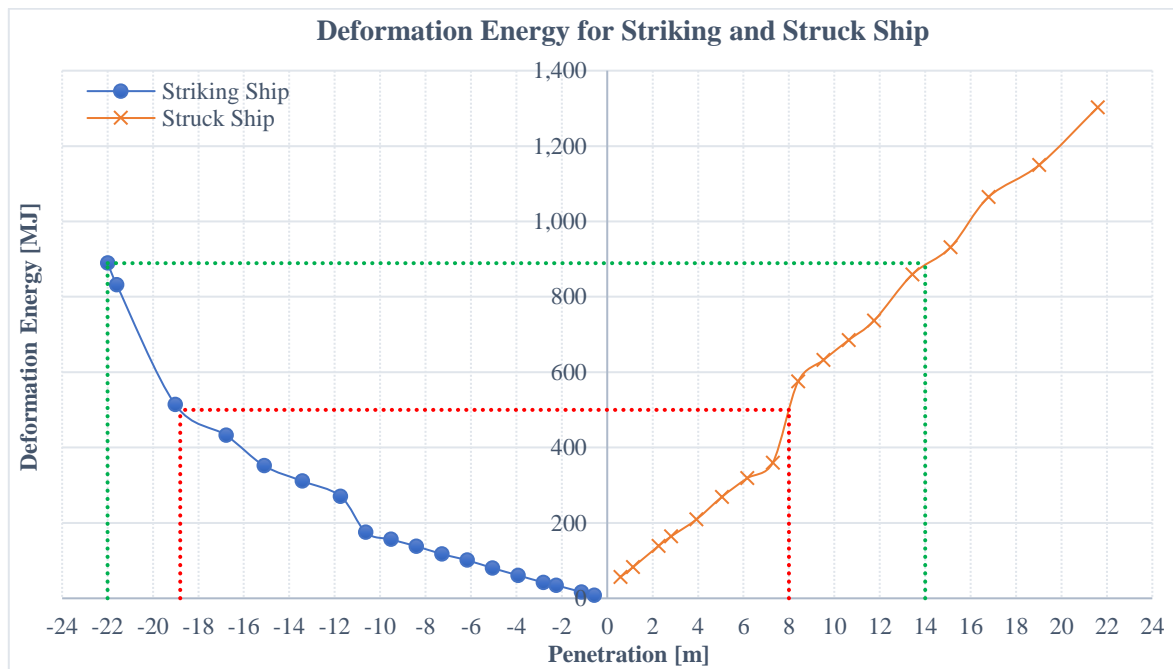
Figure 4.5. Dissipation of deformation energy in the ship-ship collision

The struck ship can absorb more deformation energy for the same penetration length compared to the striking ship. More volume is deformed in the struck ship due to its more robust impact zone. For the same rate of deformation energy, half of the initial kinetic energy is assumed to be dissipated by each ship. A reference horizontal line at 889 [MJ] leads to the penetration length at which all the kinetic energy of the striking ship impacting at 21 [knots] is equally dissipated with both models. In the struck ship, a penetration greater than 7.78 [m] from the side of the ship may lead to a catastrophic explosion event since it overpasses the gas storage limits, see Figure 4.3. While for the striking ship a complete deformation in the model length is expected.

A threshold velocity derived from the limit in the penetration length of Figure 4.5 may be suggested for a first simulation scenario. Considering a maximum penetration length of 8.0 [m] in the struck ship, 500 [MJ] would be the maximum kinetic energy both ships can dissipate in the collision considering current geometries and assumptions. Then, the initial top speed of the striking ship to get such energy is 15.5 [knots]. The striking ship model must deform 19 [m] to absorb the same amount of energy. Stiffening of plates may imply more absorbed energy for further estimation.

4.2. Generation of struck and striking ship models.

The simulation of a perpendicular high-speed collision between two ship models provided by the company is generated with LS-Dyna explicit solver. Some attention to the elements of the mesh must be given since the complexity of the mesh used may lead to not convergence in the solution. A solution conditionally stable can significantly increase the computational cost caused by a very small time-step. It is recommended this time step be less than the critical value, which is defined by the time the shock elastic wave needs to travel between the nodes of the smaller element in the mesh, moving at the velocity of the sound propagation in the material as explained in Section 2.4. The mesh of the struck ship model and the bow of the striking ship were provided by the company Chantiers de L'Atlantique for the preparation of the collision scenario. The struck ship mesh is constructed by 716617 elements among beam, shell, and mass elements, half of the section is shown in Figure 4.6. The external box-shaped dimensions are 36.8 [m] length, 47[m] width and 15.8 [m] height. The average characteristic element length of this model is 0.38 [m], nevertheless, in some plates in which openings are defined, the element size decreases up to 15 times the average and smaller time steps are expected according to Eq. 5.
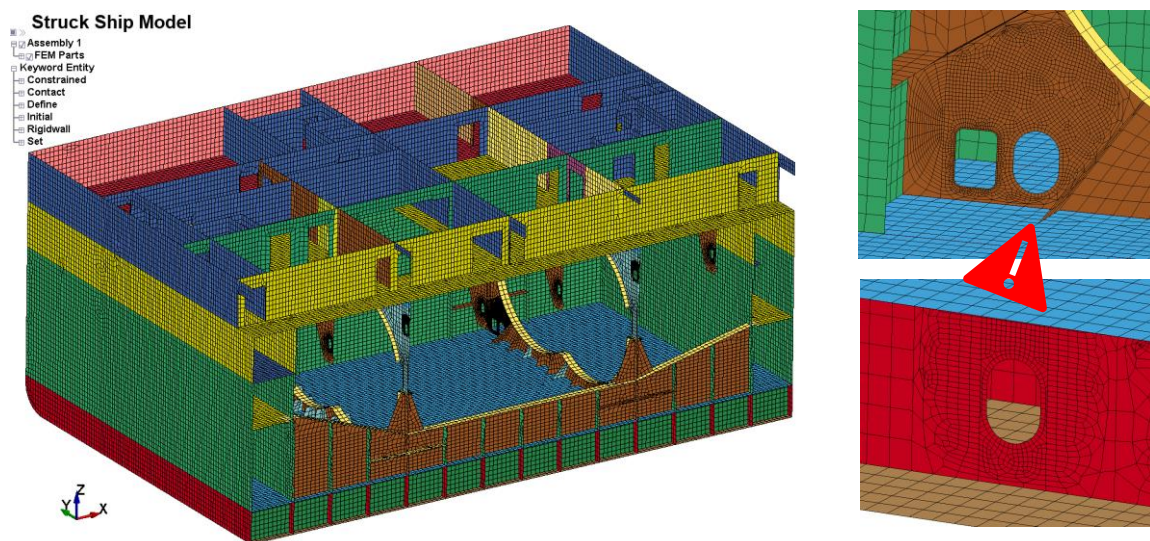
Figure 4.6. Half section of the real struck ship mesh

The striking bow is defined by a mesh with 28657 elements with an average element size of 1 [m]. A striking model with a coarser mesh than the struck one would imply overestimation in the rigidity of the striking ship. Large differences in the characteristic element length were found, see Figure 4.7. It is worth noticing, although greater elements are defined in the mesh of the striking ship, the time step is defined by the smallest element considered for the solution of the overall simulation, accounting for those of the struck mesh. This is not the case for the

elements considered as rigid in the collision since they do not participate in the time step calculation.
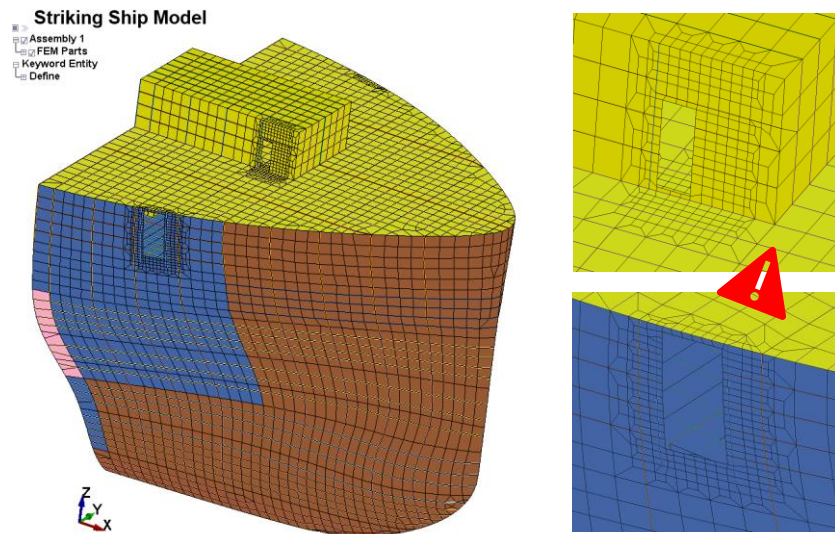
Figure 4.7. Real striking ship bow mesh

A pre-treatment of both meshes is suggested before the setting up of the collision scenario to avoid an unstable solution in the simulation. A modification of the actual meshes is the preference for the improvement of the simulation although complex structures and hull shapes involve a great pre-treatment effort. Next in order, a new mesh is modelled considering the main dimensions of the actual models and primary stiffening elements modelled as plates.

The struck ship is simplified as a box-shape with constant cross-section and only half part of it is used for the simulation since the design parameter is determined by the penetration length, in this case, see Figure 4.8a. The main stiffening system made by longitudinal and transversal plates was kept in the new model. The openings were all disregarded for the generation of a simpler mesh completely made by square elements of 0.22 [m] characteristic element length. Besides, primary stiffeners on the side shell are represented as beam elements. While only transverse stiffeners arranged for decks and transverse bulkheads are added, since are expected to deform in compression regarding the collision direction. The same thicknesses and part distribution is kept from the original mesh. Besides, an upper deck was included in the model.

(a) Half section of the struck ship   (a) Striking ship bow
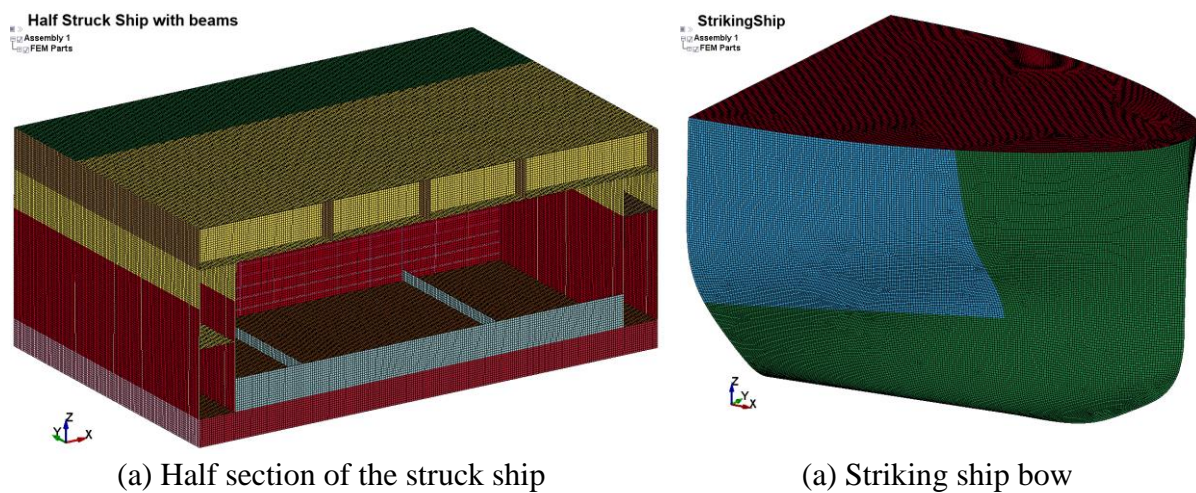
Figure 4.8. Proposed mesh models for the collision scenario

The striking ship mesh is generated considering the actual right-angle bow shape for the study of its influence in the collision. The mesh is formed by rectangular and triangular elements required to follow the curvature of the plates. The average characteristic element length for rectangular elements is 0.22 [m], while 0.15 [m] for triangular ones. As it was considered for the struck ship, the openings were disregarded for simplicity in the mesh generation. In both cases, mass elements are set up in the collision scenario file as uniformly distributed masses among all the nodes of the ship's models.

4.3. Setting up and results of the impact scenario

To analyse the structural response considering the influence of the rigid striking ship bow and striking velocities, a simulation with LS-Dyna code is set up. As described in Section 3.2.2, a third main file for controlling the collision scenario is needed. A text file describing a set of instructions called keywords is handled with mostly the same cards presented in the mentioned section. Some additional cards are described in this section for the definition of the additional mass distribution among the nodes of the models.

One additional scenario with a different striking ship is included for analysing the influence of the bow shape in the collision. The rigid striking bow shape presented in Section 3.2.1 is used to generate an additional collision scenario with the same physical properties used in that section. The struck ship is considered at rest for both cases and rigid parts must be defined in both ships for the association of the remaining inertia properties of the ship and the global dynamic response as rigid bodies simulated with the MCOL code. The speed of the striking ship for the impact of these scenarios is 21 [knots] which is the reference design velocity of the right-angle striking ship.

(a) Right-angle striking ship bow   (a) V-Shape striking ship bow

Figure 4.9. The initial position of the collision scenarios (Front view)

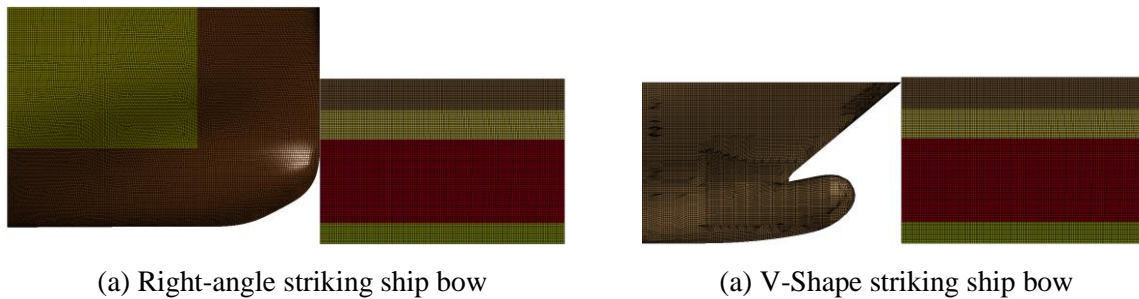Figure 4.9 is sketched the two arrangements considered for the collision scenarios to simulate. For each bow shape, one simulation is set up contemplating the striking ships as rigid, to analyse the influence of the bow shape in the collision damage. For the V-Shape striking bow, the inertia properties highlighted in the card definition of APPENDIX A1 are remaining.

An additional weight distribution corresponding to the machinery, outfitting, and structural details not considered in the mesh model, should be included for the simulation. In the previous section, the structural response of an installation under the event of the collision was defined in terms of strain energy dissipation. For this reason, only the main structural components were considered in the shapes to define the mesh of the models, however, there are many components of the auxiliary systems that may influence the global dynamic of the event. The total weight of those elements is uniformly distributed over a set of nodes belonging to the deformable parts of the struck ship. Figure 4.10 shows how two additional cards define such a task. The keywords *SET_NODE and *ELEMENT_MASS_NODE_SET are used to define the group of nodes and the total weight to be uniformly distributed among them respectively.

```
$                              Creating set of nodes for the deformable part
*SET_NODE_GENERAL_TITLE
Nodes_DeformPArt
$#     sid         da1        da2        da3        da4     solver
         1         0.0        0.0        0.0        0.0MECH
$#  option          e1         e2         e3         e4         e5         e6         e7
PART               1          2          3          4          5          6          7
PART               8          9          10         11         12         13
$
$ --------------------------------------------------------------------------
$                              Lumped mass in the nodes of the struck ship
*ELEMENT_MASS_NODE_SET
$   EID|NODE ID|            MASS|PART ID|
     1         1      2.5587E+06
$
```

Figure 4.10. Additional weight distribution on the struck ship nodes

4.3.1. Rigid right-angle striking ship bow

Complete damage in the structure of the struck ship is found after 3 [sec] of simulation. The large kinetic energy generated by the initial velocity of the striking ship produces a shrinkage effect of the struck model including the external bulkheads. The rigid part definition of the struck ship was defined in the two most external transverse floors of the model, see Figure 4.11b, however, its non-deformable restriction makes it fold the transverse bulkheads. After the collision, 65% of the initial kinetic energy remains in the system which means a small dissipation from the deformation energy in the struck ship.

<table>
<tr><td>(a) top view</td><td>(b) front view of global displacement</td></tr>
</table>
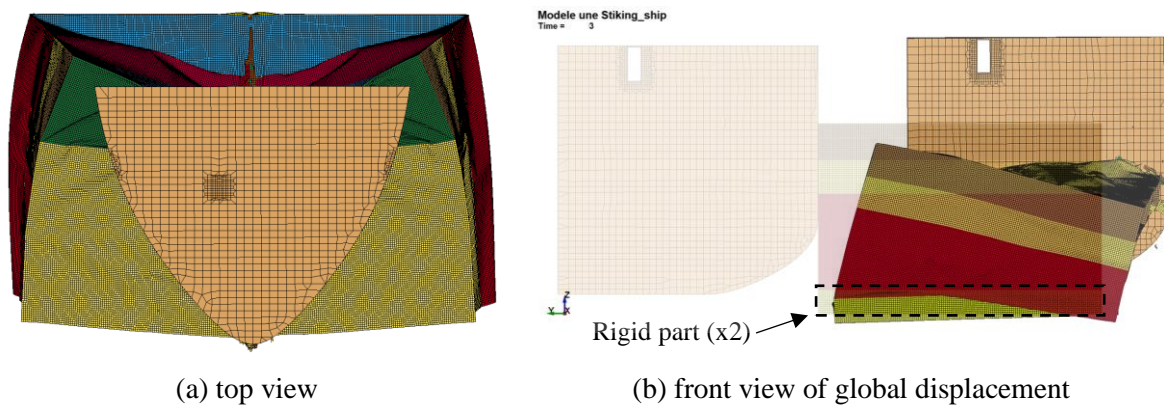
Figure 4.11. The extent of damage with rigid right-angle striking ship bow

It was observed a small rigid body global displacement of the struck ship after the impact. The large initial speed of the collision does not allow the struck structure to react to the global displacement due to the external dynamics of the bodies. At the end of the simulation, the deformation energy is 318 [MJ] and sliding energy is 148 [MJ]. As observed in Figure 4.11a, the complete penetration of 23.5 [m] was reached in the model, and the maximum internal energy is 466 [MJ]. It is found that according to the deformation energy estimated in Figure 4.5 for the struck ship, the same internal energy was expected at one-third of the current penetration length. It is worth mentioning the assumption of the crushed volume follows the deformation pattern given by the striking ship plan shown in Figure 4.3, compared to the local shaped damage volume delineated in Figure 4.11a. In addition, some small heave in the striking ship is found due to the initial draft position of both ships and more rigid structure in the double bottom of the struck ship.

4.3.2. Rigid V-Shape striking ship bow

The high initial kinetic energy and the bow shape of this scenario are the main parameters controlling the damage of the struck ship in the simulation. Complete damage of the struck ship was observed after 3 [sec] of simulation as obtained in the previous case. The sharpening surface of the striking ship broke a portion of the struck ship deck making more aggressive the collision mainly influence by the initial velocity of the striking ship, also noticing the initial position below the upper deck of the struck ship. There is similar folding behaviour of the transverse bulkheads as in the previous case, also caused by the interaction of the rigid floors located at the same position, see Figure 4.11b.

(a) top view   (b) front view of global displacement
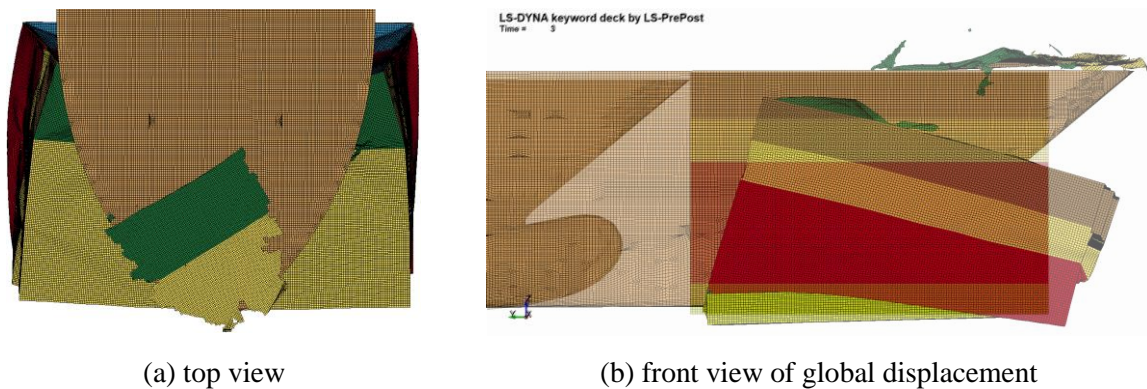
Figure 4.12. The extent of damage with rigid V-Shape striking ship

Regarding the energy dissipation, there is 63% of the initial kinetic energy remaining at the end of the simulation. The internal energy dissipated in this scenario is 356 [MJ] from deformation and 194 [MJ] from sliding energy. Complete penetration of the model is observed in Figure 4.12a, and the same localized damage volume is found compared to the estimation made in Figure 4.5. High-speed collision events are expected to be catastrophic in terms of structural damage. So far, collision scenarios have been considered with five times less initial speed than this case making some easy to analyse the deformation of different components and their contribution to the total dissipation energy. It does not worth expecting a predictable structural behaviour in such events but losses of the ship. On the other hand, the consideration of a rigid striking ship gets worse the structural damage in the deformable struck ship.

5. CONCLUSIONS

The purpose of the current study was to determine a comparison between two numerical approaches to determine the structural damage of acute-angled ship-ship collision events, considering a non-zero initial velocity of the struck ship. In the first section, a literature review about the studies of this type of accidental state evidencing the lack of information regarding the investigation of energy dissipated by friction when assessing numerical simulations and the implicit relationship between the current methods was presented. A quick review of the theoretical concepts behind the numerical tools used to investigate non-right-angle collisions was included. Secondly, a comparison of two acute-angled collisions scenarios based on finite element method and super-element approaches were developed in two stages: the setup and validation of a parametrized collision scenario comparing with a recent benchmark collision study and then the generation of narrow-angled collision scenarios considering non-zero initial velocity in the struck ship. The comparison of the new scenarios is developed with the results of penetration length and internal energy obtained with the nonlinear explicit finite element solver LS-Dyna and the super-element-based program SHARP. In the last section, one quick analytical tool is proposed for the pre-design stage focused on the assessment of the ship collision damage. The aim is to contribute to the ship construction industry, the inclusion of first some design parameters for the future crashworthiness assessment since the early stage of design. This stage was developed in collaboration with the Noise and Vibration department of the shipyard Chantiers de L'Atlantique in Saint-Nazaire France. Some findings of the study are mentioned:

5.1. Damage prediction

- There is a clear increase in the total internal energy due to the rupture criteria assumed in LS-Dyna. In the validation of the benchmark study, the contribution from deformation energy is noticeable greater when observing the time evolution response of the structure. Even though there was more correspondence in the damage extent with the maximum values, the elements of the mesh contribute with more deformation energy before it reaches the threshold strain for the rupture. This relation is clearer for right-angle collisions than oblique impacts since there is less influence from the sliding energy.

- In the cases of the acute-angled scenarios, the super-element-based SHARP program, gets smaller damage length values due to the sensitivity of more perpendicular influence than sliding impact. When both ships collide following opposite directions, LS-Dyna

simulates long damage in the side shell of the struck ship, and so does not the SHARP program but with similar indentation. Then the great influence of the sliding process is noticeable in the finite element method but not possible to determine in the super-element approach. Finally, the close-form expressions implemented in the SHARP program are limiting the evaluation of the deformation energy coming from different parts that are not being touched in the collision as the decks in this case of study. Boundary conditions assumed in the super-element approach do not allow the contribution of more strain energy coming from such elements.

- When both ships collide following the same direction, the impact is mainly influenced by the perpendicular component of the velocity regarding the struck ship. For acute-angled collisions, mostly a right-angle ship impact behave is expected to be assessed. The SHARP program evaluates a similar damage extent than LS-Dyna and it is based on the more perpendicular effect of the striking ship.

- For the shipyard Chantiers de L'Atlantique, it has been possible to propose a first quick assessment of the penetration length based on the volume of the main structural elements intended to resist the impact. Using a direct relation between the energy of deformation and the volume of damaged material, it was defined a limit for the initial kinetic energy of the striking ship. Assuming a complete dissipating of the kinetic energy on both deformable striking and struck ships, a quick first parameter for the setup of further collisions simulations was estimated. From the simulations with high initial speed, it does not worth expecting a predictable structural behaviour in such events but losses of the complete ship regardless the shape of the striking bow.

5.2. Future works and recommendations

- To better understand the influence of acute-angled angles in ship collisions, more simulations at different velocities are suggested, both for the striking and struck ships. This would help to follow the influence of the perpendicular velocity component of the striking ship for the super-element approach when both ships have the same direction. While better tracking of the sliding energy contribution with finite element method may be obtained. It would be interesting to consider different boundary conditions for the super-elements to establish some contribution in the resistance force even when the element is not touched but interacting with its connection to the edges.

- Although a rapid prediction and raw prediction of the penetration is convenient for the pre-design stage, it is cheap in terms of accuracy. It is worth noticing, no stiffeners were

included in the volume contribution for the calculation of the deformation energy. A first improvement may be to include the stiffeners that are expected to deform in plate tension and folding horizontally and vertically.

- Simulations considering both deformable ships but with the velocity derived from the rapid prediction is still under investigation. Up to this point, the rigid striking ship has been used in the collision scenarios, now following the concept of a shared-energy design, a ship collision scenario can be generated with both deformable ships. Results of several simulations may help to improve the approach by generating a type of empirical study. Finally, a good arrangement of the inertia parts must be considered for the simulations; as a first step with the generation of larger models so that the zone of interest is not being affected by the induced stiffness of the rigid parts and second to consider the global interaction of the parts to not generate unrealistic events.

6. REFERENCES

(LSTC), L. S. (2017). KEYWORD USER'S MANUAL. Livermore, California, USA.

Allianz. (2012). *Safety and Shipping.* Hamburg: Allianz. Retrieved from Allianz Global Corporate & Specialty, Safety & Shipping From Titanic to Costa Concordia: www.agcs.allianz.com/news-and-insights/

Allianz. (2019). *Allianz Global Corporate & Specialty*. Retrieved from Shipping loss and accident locations and common causes: https://www.agcs.allianz.com/news-and-insights/expert-risk-articles/shipping-safety-worst-accident-locations.html

Allianz Global Corporate & Specialty. (2019). *Allianz.* Retrieved from Allianz Global Corporate & Safety: www.agcs.allianz.com

Bela, A., Le Sourne, H., Buldgen, L., & Rigo, P. (2016). Ship collision analysis on offshore wind turbine monopile foundations. *51*.

Birol, D. F. (2019). *Offshore Wind Outlook.* IEA Publications: International Energy Agency.

Buldgen, L., Le Sourne, H., & Pire, T. (2014). Extension of the super-elements method to the analysis of a jacket impacted by a ship. *38*.

Chen, C. J., Liu, W., & Chern, S. M. (1994). *Vibration Analysis of Stiffened Plates.* Chung Cheng Institute of Technology, Department of Civil Engineering. Taiwan: Elsevier Science. Ltd.

Ehlers, S., Broekhuijsen, J., Alsos, H., Biehl, F., & Tabri, K. (2008). Simulating the collision response of ship side structures: A failure criteria benchmark study. *International Shipbuilding Progress, 55*(55).

Ferrari, A., & Rizzuto, E. (2001). *Experimental Modal Analysis of a Ship Deck Structure.* DINAV-Department of Naval Architecture & Marine Technologies. Genoa: University of Genoa.

Géradin, M., & J.Rixen, D. (2015). *Mechanical Vibrations, Theory and Application to Structural Dynamics* (Third ed.). Chichester, West Sussex, United Kingdom: John Wiley & Sons, Ltd.

International Transport Forum. (2019). *Transport Outlook.* OECD Publishing.

ISSC. (2018). Accidental Limit States. *International Ship and Offshore Structure Congress*, (p. 72).

J. Jonkman, S. B. (2009). *Definition of a 5-MW Reference Wind Turbine for Offshore System Development.* Colorado: NREL/TP-500-38060.

Jones, N. (1990). *Structural Impact.* Liverpool: Cambridge University Press.

Le Sourne, H., & al, e. (2003). LS-Dyna Applications in Shipbulding. *4th European LS-Dyna Users Conference*, (p. 16). Germany.

Le Sourne, H., & al., e. (2021). A comparison of crashworthiness methods for the assessment of ship damage extents. *Proceedings of the 1st International Conference on the Stability and Safety of Ships and Ocean Vehicles* (p. 14). Glasgow: STAB.

Le Sourne, H., Besnard, N., Cheylan, C., & Buannic, N. (2012). A Ship Collision Analysis Program Based on Upper Bound Solutions and Coupled with a Large Rotational Ship Movement Analysis Tool. *Journal of Applied Mathematics, 2021*.

Le Sourne, H., Donner, R., Besnier, F., & Ferry, M. (2001). External Dynamics of Ships-Submarine Collision. *2nd International Conference on Collision and Grounding of Ships*, (p. 8). Copenhaguen.

Le Sourne, H., Nicolas, B., Cedric, C., & Natacha, B. (2012). A Ship Collision Analysis Program Based on Upper Bound Solutions and Coupled with a Large Rotational Ship Movement Analysis Tool. *Journal of Applied Mathematics Upper Bound Solutions and Coupled with a Large Rotational Ship Movement Analysis Tool*, 28.

Le Sourne, H., Rodet, J., & Clanet, C. (2002). Crashworthiness analysis of a lock gate impacted by two different river ships. *7*.

Lehman, E., & Peschmann, J. (2002). Energy absorption by the steel structure of ships in the event of collisions. *Marine Structures 15 429–441*, 13.

Leissa, A. W. (1969). *Vibration of plates.* Washington, D.C. : National Aeronautics and Space Administration .

Liu, B., Pedersen, P. T., Zhu, L., & Shengming, Z. (2018). Review of experiments and calculation procedures for ship collision and grounding damage. *Marine Structures, 59*, 105-121.

Lützen, M., Simonsen, B. C., & Pedersen, P. T. (2000). Rapid Prediction of Damage to Struck and Striking Vessels in a Collision Event. *SSC/SNAME/ASNE Symposium.* Arlinhton.

M.L, K., & P, R. (2018). ACCIDENTAL LIMIT STATES. *International Ship and Offshore Structures Congress*, 72.

Minorsky, V. U. (1958). *AN ANALYSIS OF SHIP COLLISIONS WITH REFERENCE TO PROTECTION OF NUCLEAR POWER PLANTS.*

NORSOK Standard N004. (2004). *Design of Steel Structures.* Norway: NORSOK.

Pedersen, P. T. (1995). *Collision ang Grouding Mechanics.* Denmark: Technical University of Denmark.

Perdesen, P. T., & Zhang, S. (1998). On Impact Mechanics in Ship Collisions. *Marine Structures.*

Petersen, M. J. (1982). Dynamics of Ship Collision. *Ocean Engineering*, 295-329.

Pire, T. (2018). *Crashworthiness of offshore wind turbine jackets based on the continuous element method.* Liege: University of Liege.

Simonsen, B. C., & Lauridsen, L. P. (2000). Energy absorption and ductile failure in metal sheets under lateral indentation by a sphere. *International Journal of Impact Engineering 24 1017-1039*, 23.

Sone Oo, Y. (2017). *Numerical and analytical simulations of in-shore ship collisions withing the scope of ADN Regulations.* Carquefou: EMSHIP-ICAM-ECN.

Umunnakwe, C. B. (2020). *Numerical Simulations of ship grounding by taking into considerations external hydrodynamic forces.* Nantes.

Warburton, G. (1954). The Vibration of Rectangular Plates. *Proceedings of the Institution of Mechanical Engineers*, 371-384.

Zhang, S. (1999). *The mechanics of Ship Collisions.* Denmark: Technical University of Denmark.

A. APPENDIX A1

SETTING UP OF A COLLISION SCENARIO

Different data blocks that contain similar information are defined after the input of a new keyword called with the asterisk symbol '*****'. Then 80 columns are available for the data input detailed in the user manual of LS-Dyna regarding the specified keyword. Statements mentioned after '**$**' will be omitted. Data blocks may be clustered in any part of the text file and the special keyword *END will terminate the data input. The main keywords that control the initial conditions and summary of results are presented in this sub-section.

The simulation text file is divided into six blocks of data associated with the relevant keywords *CONTROL, *DATABASE, *BOUNDARY, *CONTACT, *PART and *SECTION, *MATERIAL and *INCLUDE_TRANSFORM. All of these are briefly described in the following section to keep a logical sense for user handling.

Control cards

The control cards are optional and can be defined to change default active solutions in the simulation. The user manual describes in detail the function of each control card and some additional control over the elements in the solution that may be applied with cards such as * CONTROL_TIMESTEP or * CONTROL_SHELL. However, it is mandatory to define at least the card *CONTROL_TERMINATION to stop the simulation, see Figure A.1. Six values between floating and integer are required to define this card.

```
*CONTROL_TERMINATION
$  ENDTIM|   ENDCYC|    DTMIN|   ENDENG|   ENDMAS|   NOSOL|
 8.0000000         0 0.0000000 0.0000000 0.0000000        0
```

Figure A.1. Definition of the simulation time

For the validation of the collision scenario, the simulation was requested to stop after 8.0 [sec]. The additional fields are set as a default value of 0 since it is no termination cycle or reduction of the time step is required. More details of this card and further omitted fields can be found in the LS-Dyna Keyword User's Manual, Volume I (2017).

Output cards

Define output cards with database keywords is optional but also needed to obtain information from the collision in the function of the time simulation. Besides the numerical results, sketching of the crushing process with a set of plots with a certain frequency can be generated with the cards *DATABASE_BINARY_D3PLOT and *DEFINE_CURVE. A total of 100 plots

are used to describe the crushing process. Energy results for a global state and individual parts of the structures are saved parallelly with *DATABASE_GLSTAT and *DATABASE_MATSUM respectively.

Boundary cards (MCOL coupling)

The internally integrated MCOL code allows emulating the dynamics of ships through a rigid body mechanics program. The keyword *BOUNDARY_MCOL couples the prediction of the external dynamic with the hydrodynamic information loaded from an external file to a specific part number on each ship. A maximum time step should be specified to MCOL to terminate the calculation if the code exceeds this number. All this information is detailed in the text file as shown in Figure A.2.

```
*BOUNDARY_MCOL
$ how many files will be called from MCOL
$   NMCOL|   MXSTEP| ENDTMCOL|    TSUBC|  PRTMCOL|
         2   2000000       0.0      0.1 5.000E-03
$ Specify part number and name of the file
$  RBMCOL|             MCOLFILE|
        17              DRoPax.mco
         6 floodstandShipB.mco
```

Figure A.2. Link-up of external files with Boundary MCOL

Two cards with the information for the liking are specified for this collision scenario. In the first card, two ships for the loading of the external files are allocated in the field NMCOL, followed by the specification of the maximum time step in MCOL calculation. The uncoupling termination time ETMCOL is set as default to have the same termination time of LS-Dyna. A sub cycling of 0.1 is specified in TSUBC and the field PRTMCOL is the time interval at which MCOL rigid body data will provide outputs. In the second card is detailed one by one the part and the external ***.mco** file to associate with. In the column named RMBCOL a rigid body part number **17** of the striking ship is linked with the external hydrostatic parameters **DRoPax.mco** that was generated with a 3D seakeeping software.

Contact cards

To establish the physical interaction of the elements of the mesh that are being collided, contact cards must be specified. Two types of contacts are required to simulate the physical interaction: A global one between ship and ship and another for the internal components of each ship. The card *CONTACT_AUTOMATIC_SURFACE_TO_SURFACE is made up of three rows of fields to specify the contact, see Figure A.3, however, only Master and Slave elements must be identified to slide with a certain static and dynamic coefficient of friction. These latter are in the second row within the fields FS and FD respectively and both at 0.3.

```
*CONTACT_AUTOMATIC_SURFACE_TO_SURFACE
$     SSID|     MSID|    SSTYP|    MSTYP|   SBOXID|   MBOXID|       SPR|       MPR|
          1        17         2         3         0         0         0         0
$       FS|       FD|       DC|       VC|      VDC|   PENCHK|        BT|        DT|
  0.3000000 0.3000000 0.0000000 0.0000000 0.0000000         0 0.0000000 0.0000000
$      SFS|      SFM|      SST|      MST|     SFST|     SFMT|       FSF|       VSF|
  0.0000000 0.0000000 0.0000000 0.0000000 0.0000000 0.0000000
          0 0.0000000         0 0.0000000 0.5000000         0         0         0
```

Figure A.3. Contact card for ship-ship interaction

The struck ship is being represented by a set of deformable and rigid parts while striking is considered as a single rigid surface directly set as the master part in MSID. On the other hand, one single slave part is set in SSID which is a group of all the deformable parts of the struck ship. The card *SET_PART is used in this section to group shell and beam elements and later be used under ID number 1. The difference between the use of Parts and Part Sets for this card is done in the SSTYP and MSTYP fields for slave and master elements respectively.

An automatic self-contact between all the deformable elements of the struck ship is also required when they get in touch. This is specified with the card *CONTACT_AUTOMATIC_GENERAL that is defined with a given ID number. Similarly, to the previous card, slave and master elements should be identified in this section, but also the already defined Part Set 1 may be used. Denoting only as Slave Part Set number 1 with no Master element, the self-contact of the deformable parts will be considered. Static and dynamic frictional coefficients are also set as 0.3 in this section.

Part and section cards

The definition of Parts related to a specific Section converts the geometry into a structural model. When Struck and Striking ship meshes were defined in Section 3.2.1, each shell and beam element was associated with a specific Part Number to denote the similarity of their physical properties. The keyword *PART defines the name and the connection of the element with an already defined dimension with the card *SECTION as shown in Figure A.4 for all shell elements of the side shell.

```
$                              Struck ship side shell
*PART
$#                                                                   title
SideShell
$#     pid     secid       mid     eosid      hgid      grav    adpopt      tmid
         1         1         1         0         0         0         0         0
$
*SECTION_SHELL_TITLE
Section_SideShell
$#   secid     elform      shrf       nip     propt   qr/irid     icomp     setyp
         1        16       0.0         5       0.0         0         0         0
$#      t1        t2        t3        t4      nloc     marea      idof    edgset
     0.015     0.015     0.015     0.015       0.0       0.0       0.0         0
```

Figure A.4. Definition of Side Shell properties

In the first card, all the shell elements with Part ID 1 will have the thickness specified in Section 1 and the characteristics of Material ID 1. In the second row, the card *SECTION_SHELL or *SECTION_BEAM could be used according to the elements referred to in the mesh. For the side shell, a thickness of 15 [mm] is set. A total of 5 integration points for the finite element solution is defined in NIP. The element formulation ELFORM defined is EQ.16 which refers to Fully Integrated shell elements (very fast). Suggestion to this formulation was made to reduce the Hourglass energy since less than 10% of the maximum total energy must be kept.

Beam elements are defined between every two nodes and linked with the parts of the shell elements. The card *INTEGRATION_BEAM is used to define the beam elements through the thickness integration rules and connected with the card *SECTION_BEAM to define the shape of the beam. Different parts containing only beam elements are created following the shell parts presented in Figure 3.4.

The rigid part definition should be done in such a way that in combination with the deformable parts the real ship representation is obtained. In the case of the Struck Ship, the rigid part is located at the two extreme bulkheads of the model, as shown in Figure 3.4. These parts will contain the information of the centre of gravity, mass, and inertia of the Struck Ship with some corrections to consider the deformable sections and complete the ship in the global frame of reference. By knowing the information of the real inertia of the ship around each axis, the inertia of the rigid part can be obtained with Eq. 18. This information is obtained from the MCOL data provided and with the d3hsp file generated in the simulation.

$$I_{xx}{}^{Ship} = I_{xx}{}^{deformable} + I_{xx}{}^{rigid} \qquad \text{Eq. 18}$$

The same procedure applies for the inertia properties around the other axis and is similar for the centre of gravity with the equilibrium of moments. The directional orientation of the real ship in surge and sway is defined by the vectors of the last row as shown in Figure A.5. Also, an arbitrary rigid thickness is specified although no participation in the solution is related to this information but required for the finite element method. The initial velocity of the rigid parts is defined as 0 in the parameter VELA since the ship is considered at rest for this validation. In the case of nonzero velocity, the Part Inertia and the nodes of the deformable parts should be set with the same initial velocity. This collision file was prepared in such a case for future scenarios where both ships are moving.

```
*PART_INERTIA
Struck_ship_rigid_part
$      PID|     SECID|       MID|     EOSID|     HGID|      GRAV|    ADPOPT|      TMID|
          6         6         5         0         0         0         0         0
$       XC|        YC|        ZC|        TM|     IRCS|    NODEID|
      35.63.0372E-01    -0.17  32752408         1
$      IXX|       IXY|       IXZ|       IYY|      IYZ|       IZZ|
4.0613E+09        0.0       0.01.2148E+11        0.01.2564E+11
$      VTX|       VTY|       VTZ|       VRX|      VRY|       VRZ|
     &VELA        0.0       0.0       0.0       0.0       0.0
$       XL|        YL|        ZL|      XLIP|     YLIP|      ZLIP|       CID|
      1.0         0.0       0.0       0.0       1.0       0.0
*SECTION_SHELL_TITLE
Section_Rigid
$#   secid    elform      shrf       nip     propt    qr/irid     icomp     setyp
         6         0       0.0         0       0.0         0         0         0
$#      t1        t2        t3        t4      nloc     marea      idof    edgset
     0.007     0.007     0.007     0.007       0.0       0.0       0.0         0
```

Figure A.5. Rigid part definition for the struck ship

In the case of the striking ship, the single surface is considered as a rigid part and contains the information of the complete ship. The centre of gravity, mass, and inertia is corresponding to the complete ship with no correction. Besides, the velocity is set with the parameters denoted in Figure 3.6. Surge and Sway directions are parametrized also with the information given in the definition of the initial conditions of the striking ship. Then velocity vectors and position of the centre of gravity change when non-right-angle collision are considered, being consistent with the global frame of reference.

Material cards

As mentioned in the Keyword User's Manual, Volume II (2017), LS-Dyna refers to each material model by a number. A wide set of instructions to describe the behaviour of a material can be used especially when non-linear studies are assessed. The failure strain criteria vary according to Eq. 6 suggested by (Lehman & Peschmann, 2002), where the ratio between thickness and equivalent length of the element determines the strain threshold for the numeric calculation. However, it was also observed by (Simonsen & Lauridsen, 2000) when there is an important influence of the shell element dimension, an asymptotic value of 0.2 for the plastic strain should be considered.

The ratio element-thickness for all the elements of this simulation is greater than 13 and the formulation suggested in Eq. 6 is not convenient for having realistic behaviour. Then, all the failure strain of the materials for the struck ship are set as 0.2 in the FAIL field of the card *MAT_PIECEWISE_LINEAR_PLASTICITY to prevent the big erosion of the shell elements of the simulation. Only the first row of input data for the material definition of the side and bottom shell elements is presented in Figure A.6 since the same thickness is considered for certain plates.

```
$                                              Material for SIDE SHELL and BOTTOM
*MAT_PIECEWISE_LINEAR_PLASTICITY
$     MID|        RO|         E|        PR|      SIGY|      ETAN|      FAIL|      TDEL|
        1 7800.0000 2.0038+11 0.3000000 255.000+6 1.00000+7       0.2 0.0000000
```

Figure A.6. Material for Side and Bottom plates

Bilinear plastic behaviour of the steel is defined by the ETAN modulus from the elastic limit SIGY up to the end of the plastic strain. Rigid materials are also defined for the finite element calculation with the card *MAT_RIGID.

Transformation cards

The importation and positioning of the ship meshes into the main collision file are done with the transformation cards. Usually, the meshes are generated separately and the ID of nodes and elements are assigned starting from 1. To avoid the overlapping of the same identification numbers in the main file when meshes are imported an offset for all nodes, elements, and parts in one of them may be applied with the card *INCLUDE_TRANSFORM. The name of the external file is specified and the initial ID offset for all the elements to be imported. The transformation is associated with a transformation ID that may be used with *DEFINE_TRANSFORMATION card to rotate and translate the mesh in the global frame of reference. For the striking ship, using two points a vector is defined to rotate the ship about the bow of the ship.
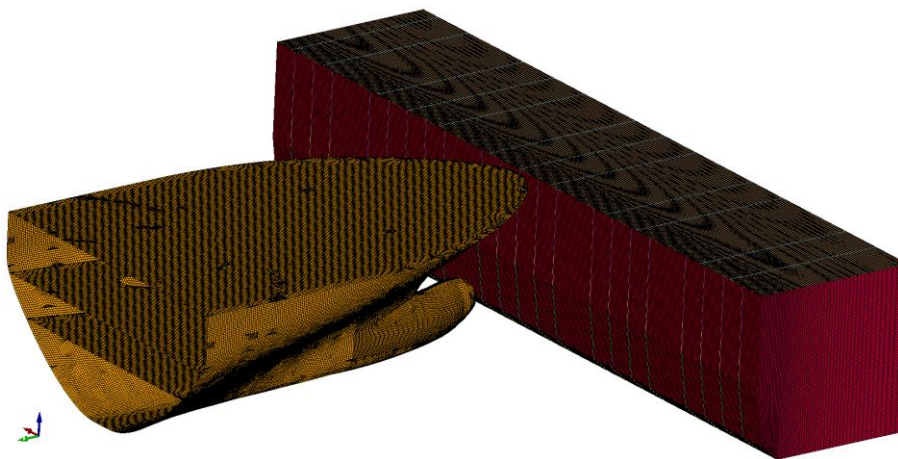

Figure A.7. The general arrangement of the collision scenario

Finally, the main collision scenario file is generated and tested with some simulations to validate it regarding the benchmark collision study. A certain allowance between the meshes while locating the striking ship is strictly necessary to avoid any initial penetration but also for saving some simulation time as shown in Figure A.7. A general idea was to consider it is enough to have an allowance slightly bigger than the sum of half of the thickness of the plates to impact in the collision point.